MIT Open Access Articles

Search for supersymmetry in pp collisions at √ s = 8 TeV in events with a single lepton, large jet multiplicity, and multiple b jets

Massachusetts Institute of Technology

Search for supersymmetry in pp collisions at $\sqrt{s} = 8$ TeV in events with a single lepton, large jet multiplicity, and multiple b jets

CMS Collaboration⋆

CERN, Switzerland

A B S T R A C T

Results are reported from a search for supersymmetry in pp collisions at a center-of-mass energy of 8 TeV, based on events with a single isolated lepton (electron or muon) and multiple jets, at least two of which are identified as b jets. The data sample corresponds to an integrated luminosity of 19.3 fb^{-1} recorded by the CMS experiment at the LHC in 2012. The search is motivated by supersymmetric models that involve strong-production processes and cascade decays of new particles. The resulting final states contain multiple jets as well as missing transverse momentum from weakly interacting particles. The event yields, observed across several kinematic regions, are consistent with the expectations from standard model processes. The results are interpreted in the context of simplified supersymmetric scenarios with pair production of gluinos, where each gluino decays to a top quark–antiquark pair and the lightest neutralino. For the case of decays via virtual top squarks, gluinos with a mass smaller than 1.26 TeV are excluded for low neutralino masses.

© 2014 The Authors. Published by Elsevier B.V. This is an open access article under the CC BY license (http://creativecommons.org/licenses/by/3.0/). Funded by SCOAP^3.

1. Introduction

This paper presents results from a search for new physics in proton–proton collisions at a center-of-mass energy of 8 TeV in events with a single lepton (electron or muon), missing transverse momentum, and multiple jets, at least two of which are tagged as originating from bottom quarks (b-tagged jets). This signature arises in models based on supersymmetry (SUSY) [1–6], which potentially offers natural solutions to limitations of the standard model (SM). Large loop corrections to the Higgs boson mass could be cancelled by contributions from supersymmetric partners of SM particles. Achieving these cancellations requires the gluino ($\tilde{g}$) and top squark ($\tilde{t}$), which are the SUSY partners of the gluon and top quark, respectively, to have masses less than about 1.5 TeV [7–10]. Here and throughout this document we only consider the lighter of the two top squarks. Extensive searches at LEP, the Tevatron, and the Large Hadron Collider (LHC) have not produced evidence for SUSY (see Refs. [11–17] for recent results in the single-lepton topology). For scenarios with mass-degenerate scalar partners of the first- and second-generation quarks, the mass limits generally lie well above 1 TeV. However, viable scenarios remain with $\tilde{t}$ and $\tilde{g}$ masses below approximately 0.5 and 1.5 TeV, respectively.

In some of these scenarios top squarks are the lightest quark partners. In R-parity conserving models [18] this could lead to signatures with multiple W bosons, multiple b quarks, and two LSPs in the final state, where the LSP is the weakly interacting lightest SUSY particle. The search described in this paper is designed to detect these signatures. It focuses on gluino pair production, with subsequent gluino decay to two top quarks and the LSP ($\tilde{\chi}_1^0$) through either a virtual or an on-shell top squark: $pp \rightarrow \tilde{g}\tilde{g}$ with $\tilde{g}(\rightarrow \tilde{t}\bar{t}) \rightarrow t\bar{t}\tilde{\chi}_1^0$. These decay chains result in events with high jet multiplicity, four b quarks in the final state, and large missing transverse momentum ($\not{E}_T$). The probability that exactly one of the four W bosons decays leptonically is approximately 40%, motivating a search in the single-lepton channel.

Three variations of this scenario, denoted as models A, B, and C, are considered in this analysis and implemented within the simplified model spectra (SMS) framework [19–21]. In model A (models B and C), gluinos are lighter (heavier) than top squarks and gluino decay proceeds through a virtual (real) $\tilde{t}$. For model A, the gluino and LSP masses $m_{\tilde{g}}$ and $m_{\tilde{\chi}_1^0}$ are allowed to vary. For model B, we set $m_{\tilde{g}} = 1$ TeV and vary $m_{\tilde{\chi}_1^0}$ and the top squark mass $m_{\tilde{t}}$. For model C, $m_{\tilde{\chi}_1^0} = 50$ GeV while $m_{\tilde{g}}$ and $m_{\tilde{t}}$ are varied.

The relevant backgrounds for this search arise from $t\bar{t}$, W + jets, and single-top quark processes with small contributions from diboson, $t\bar{t}Z$, $t\bar{t}W$, $t\bar{t}H$, and Drell–Yan (DY) + jets production. The non-$t\bar{t}$ backgrounds are strongly suppressed by requiring at least six jets,

at least two of which are b-tagged. The remaining background is dominated by $t\bar{t}$ events with large $\not{E}_T$, generated either by a single highly boosted W boson that decays leptonically (single-lepton event) or by two leptonically decaying W bosons (dilepton event). Though $t\bar{t}$ decays produce two true b quarks, additional b-tagged jets can arise because of gluon splitting to a $b\bar{b}$ pair or from mistagging of charm-quark, light-quark, or gluon jets.

We search for an excess of events over SM expectations using two approaches. The first approach is based on the distribution of $\not{E}_T$ in exclusive intervals of H_T, where H_T is the scalar sum of jet transverse momentum (p_T) values. In this approach, we evaluate the $\not{E}_T$ distribution in the signal region of high H_T in two different ways [12,13]: by extrapolating from lower H_T and by using the charged-lepton momentum spectrum (this latter spectrum is highly correlated with the neutrino p_T spectrum in events with a leptonically decaying W boson and so carries information about $\not{E}_T$). In this approach combined signal regions for the e and the μ channels are used since the differences in terms of backgrounds and sensitivity are small.

The second approach, which is new and described in more detail in this paper, is based on the azimuthal angle, $\Delta\phi(W, \ell)$, between the reconstructed W-boson direction and the lepton. The single-lepton background from $t\bar{t}$ is suppressed by rejecting events with small $\Delta\phi(W, \ell)$. As will be shown later, this angle carries information similar to the transverse mass of the lepton and $\not{E}_T$, but has superior resolution. The search is performed in different regions of the quantity S_T^{lep}, defined as the scalar sum of the $\not{E}_T$ and lepton p_T. The S_T^{lep} variable is a measure of the leptonic energy in the event and does not necessarily require high $\not{E}_T$ in order to be large. SUSY events are expected to appear at large S_T^{lep}, where the contribution from SM processes is small. The definition of signal regions in terms of S_T^{lep} allows the inclusion of events with lower $\not{E}_T$ than are included in the first approach. Therefore the e channel receives a small, but non-negligible correction for the presence of multijet events, and the e and the μ channels are treated as separate signal regions.

The two approaches are complementary in the kinematic observables used and data samples exploited. The first approach searches the tails of the single-lepton $t\bar{t}$-dominated sample at high $\not{E}_T$ and H_T with two independent methods, while the second approach uses $\Delta\phi(W, \ell)$ to reject that background process and search in a low-background region dominated by dilepton events in which one lepton is not identified or lies outside the acceptance of the analysis. Together the two approaches provide a broad view of possible deviations from the standard model.

2. Data sample and event selection

The data used in this search were collected in proton–proton collisions at $\sqrt{s} = 8$ TeV with the Compact Muon Solenoid (CMS) experiment in 2012 and correspond to an integrated luminosity of 19.3 fb^{-1}. The central feature of the CMS apparatus is a superconducting solenoid, providing a magnetic field of 3.8 T. Within the superconducting solenoid volume are a silicon pixel and strip tracker, a lead tungstate crystal electromagnetic calorimeter, and a brass-scintillator hadron calorimeter. Muons are measured in gas-ionization detectors embedded in the steel flux-return yoke outside the solenoid. Extensive forward calorimetry complements the coverage provided by the barrel and endcap detectors. The origin of the CMS coordinate system is the nominal interaction point. The polar angle θ is measured from the counterclockwise beam direction and the azimuthal angle ϕ (in radians) is measured in the plane transverse to the beam axis. The silicon tracker, the muon systems, and the barrel and endcap calorimeters cover

the regions $|\eta| < 2.5$, $|\eta| < 2.4$, and $|\eta| < 3.0$, respectively, where $\eta = -\ln[\tan(\theta/2)]$ is the pseudorapidity. A detailed description of the CMS detector can be found elsewhere [22].

Simulated event samples based on Monte Carlo (MC) event generators are used to validate and calibrate the background estimates from data and to evaluate the contributions for some small backgrounds. The MADGRAPH 5 [23] generator with CTEQ6L1 [24] parton distribution functions (PDFs) is used for $t\bar{t}$, W + jets, DY + jets, $t\bar{t}Z$, $t\bar{t}W$, and multijet processes and the POWHEG 1.0 [25] generator for single-top-quark production. The PYTHIA 6.4 [26] generator is used to generate diboson and $t\bar{t}H$ samples and to describe the showering and hadronization of all samples (the Z2* tune [27] is used). The cross sections used to scale the yields of these samples are calculated at next-to-leading (NLO) or higher order. Decays of τ leptons are handled by TAUOLA [28]. The GEANT4 [29] package is used to describe the detector response.

The SUSY signals for the three scenarios considered in this analysis are generated with MADGRAPH and CTEQ6L1 PDFs. In these scenarios, gluinos are pair-produced and decay into $t\bar{t}\tilde{\chi}_1^0$, assuming the narrow-width approximation. For the signal samples, the detector response is described using a fast simulation [30]. The fast simulation has been validated extensively against the detailed GEANT4 simulation for the variables relevant for this search and efficiency corrections based on data are applied. All simulated events are reweighted to match the multiplicity distribution of additional proton–proton collisions ("pileup") as observed in data.

Events are selected online with either triple- or double-object triggers. The triple-object triggers require a lepton with $p_T > 15$ GeV, together with $H_T > 350$ GeV and $\not{E}_T > 45$ GeV. The double-object triggers, which are used to select control samples and extend the $\not{E}_T$ acceptance in the approach based on $\Delta\phi(W, \ell)$, have the same H_T requirement, no $\not{E}_T$ requirement, and a lepton p_T threshold of 40 GeV. The trigger object efficiencies are measured in independently triggered control samples and found to reach a plateau at approximately 95% for thresholds well below those used in the offline selection. The measured trigger efficiencies are used to correct the simulation.

The preselection of events is based on the reconstruction of an isolated lepton (e or μ) and multiple jets and follows the procedure described in Ref. [12]. Events are required to include at least one lepton with $p_T > 20$ GeV and $|\eta| < 2.5$ (e) or $|\eta| < 2.4$ (μ). Standard identification and isolation requirements [31,32] are applied to reject backgrounds from jets mimicking the lepton signature and from non-prompt leptons produced in semileptonic decays of hadrons within jets. The isolation selection requires the sum of transverse momenta of particles in a cone of radius $\sqrt{(\Delta\eta)^2 + (\Delta\phi)^2} = 0.3$ around the electron (muon) direction, divided by the p_T of the lepton itself, to be less than 0.15 (0.12). The lepton efficiencies are measured with a "tag-and-probe" technique [33] to be approximately 80% for electrons and 95% for muons. The efficiencies vary by less than 20% over the selected kinematic range and the average values agree to better than 1% between data and simulation.

Jets are clustered from particles reconstructed with the particle-flow (PF) algorithm [34], which combines information from all components of the detector. The clustering is performed with the anti-k_T clustering algorithm [35] with a distance parameter of 0.5. Jet candidates are required to satisfy quality criteria that suppress noise and spurious non-collision-related energy deposits. Jets with $p_T > 40$ GeV and $|\eta| < 2.4$ are considered in the analysis and are used to determine the number of selected jets N_j and H_T. The missing transverse momentum is determined from the vector sum of the momenta of all particles reconstructed by the PF algorithm. Jet and $\not{E}_T$ energies are corrected to compensate for shifts in the

jet energy scale and the presence of particles from pileup interactions [36].

The number of b-tagged jets, N_b, is determined by applying the combined secondary vertex tagger [37,38] to the selected jets. At the working point used, this tagger has a roughly 70% b-tag efficiency, and a mistag rate for light partons (charm quarks) of approximately 3% (15–20%). Scale factors for the efficiencies and mistag rates relative to simulation are measured with control samples in data and applied in the analysis.

As the signal events are expected to exhibit a high level of hadronic activity and contain a large number of b quarks, events are required to have $H_T > 400$ GeV. In addition, at least two b-tagged jets and a total jet multiplicity $N_j \geq 6$ are required. The SM background in this sample is dominated by $t\bar{t}$ production. Samples selected with the requirements $3 \leq N_j \leq 5$ or $N_b < 2$ are used to define background-dominated control regions. Events with a second isolated lepton with $p_T > 15$ GeV are vetoed by the nominal signal selection to suppress contributions from dilepton $t\bar{t}$ decays, but such events are used as a control sample to measure the residual background from that process.

3. Search in missing transverse momentum and H_T

We now describe the background estimation method based on the evaluation of the $\not{E}_T$ spectrum. This method utilizes two techniques, as mentioned above, both of which were employed for previous CMS studies [12,13]. The *lepton spectrum* (LS) method makes use of the similarity between the neutrino and charged-lepton p_T spectra in W decays to predict the high-side tail of the $\not{E}_T$ distribution from single-lepton $t\bar{t}$ decays based on the p_T distribution of charged leptons with high p_T [39]. The contributions from dilepton and τ lepton decays are predicted from single-lepton and dilepton control samples. The *missing transverse momentum template* (MT) method uses a parametric description of the $\not{E}_T$ spectrum based on a fit to control regions at low H_T. Through extensive use of data control samples, we avoid uncertainties related to potential mismodelling of SM yields by the simulation in the high H_T and high $\not{E}_T$ tails.

We consider overlapping signal regions corresponding to lower limits for H_T ranging from 400 to 1000 GeV, each of which provides sensitivity to a different SUSY-particle mass region. The $\not{E}_T$ spectrum in these samples is divided into exclusive ranges: 150–250, 250–350, 350–450, and >450 GeV. To increase the sensitivity, the search regions are further divided into events with $N_b = 2$ and ≥ 3. The two background estimation methods provide direct predictions for events with two b-tagged jets. The expected yields at higher N_b are obtained by extrapolating those predictions to the ≥ 3 b-jet case.

3.1. Prediction of the single-lepton background for the LS method

The $\not{E}_T$ spectrum of the single-lepton background is predicted with a method based on the similarity of the neutrino and charged lepton p_T spectra in W decays. In each event, the charged and neutral lepton p_T can be very different, but the distributions of the true neutrino p_T and the true lepton p_T are identical in the absence of W polarization. There are several effects that result in differences between the observed lepton and neutrino p_T spectra and for which corrections are derived: W polarization, the effect of a lepton p_T threshold, and the difference between the $\not{E}_T$ and lepton-p_T resolutions. The W-boson polarization in $t\bar{t}$ decays is the dominant effect that causes a difference between the neutrino and lepton p_T spectra. This polarization is well understood theoretically [40] and accounted for in the simulation. The difference between the $\not{E}_T$ and lepton-p_T resolution is modeled with

$\not{E}_T$ resolution templates measured in multijet data samples. These samples are used because the $\not{E}_T$ resolution is dominated by the measurement of the hadronic activity in an event, and these samples have little genuine $\not{E}_T$. These resolution templates are binned in H_T and N_j and are used to smear the lepton-p_T spectrum to account for the difference with respect to the $\not{E}_T$ resolution.

The single-lepton $\not{E}_T$ spectrum is predicted from the lepton p_T spectrum using the following steps. First, the lepton p_T spectrum in a control sample, selected with lepton $p_T > 50$ GeV and without a $\not{E}_T$ requirement, is smeared with the resolution templates. The smeared distribution is then corrected with p_T-dependent scale factors κ_{LS} to obtain a predicted $\not{E}_T$ spectrum. These scale factors are defined by $\kappa_{LS}(p_T \text{ bin}) = N_{true}(\not{E}_T \text{ bin})/N_{pred}(p_T \text{ bin})$, where N_{pred} is the MC yield in a given bin of the smeared p_T distribution and N_{true} is the MC yield in the same bin of $\not{E}_T$. The latter includes only events with a single lepton at generator level, while the former includes all events passing the selection of the control sample. This definition ensures that the scale factors model the $\not{E}_T$ distribution from only the single-lepton background without contributions from τ leptons or dilepton backgrounds, which are predicted separately. The calculation of the scale factor is dominated by the contributions of $t\bar{t}$ events, but W + jets, DY + jets, single-top quark, $t\bar{t}Z$, and $t\bar{t}W$ events are included as well; the contribution of diboson events is negligible. The impact of $t\bar{t}Z$, $t\bar{t}W$, and $t\bar{t}H$ events is insignificant, and for the results shown in this section only the first two categories have been included. The dependence of the scale factor on lepton p_T primarily reflects the effect of the W-boson polarization in $t\bar{t}$ decays. The scale factor varies from around 1.0 for lepton p_T of 150 to 250 GeV, after $\not{E}_T$ resolution smearing, to about 1.5 for $p_T > 450$ GeV.

Systematic uncertainties are evaluated by calculating the change induced in the scale factors from various effects and propagating this change to the predicted yields. The sources of systematic uncertainty are the jet and $\not{E}_T$ scale, W polarization in $t\bar{t}$ decays and direct W production, $t\bar{t}$ and sub-dominant background cross sections, lepton efficiency, muon p_T scale, and DY + jets yield. The dominant uncertainties arise from the statistical uncertainties of the simulated samples used in the determination of the scale factor (9–49%), the jet and $\not{E}_T$ scale (7–31%, depending on H_T and $\not{E}_T$), and the W polarization in $t\bar{t}$ decays (2–4%).

3.2. Predictions of τ lepton and dilepton backgrounds for the LS method

Neutrinos from τ lepton decays cause the $\not{E}_T$ and charged-lepton p_T spectra to differ. Therefore, the SM background from τ leptons is evaluated separately, following the procedure documented in Ref. [39]. While τ-lepton decays are well simulated, their p_T spectra may not be. Thus we apply τ-lepton response functions derived from simulated $t\bar{t}$ events to the p_T spectra of electrons and muons measured in single-lepton and dilepton control samples. To suppress DY events in these control samples, same flavor dilepton events are rejected if they have $\not{E}_T < 40$ GeV or a dilepton invariant mass within 20 GeV of m_Z. In these control samples, the $\not{E}_T$ requirement is removed and a selection to reject DY events is applied. The H_T and N_j requirements are loosened in the control sample used to estimate the background of events with hadronically decaying τ leptons. For leptonic (hadronic) τ-lepton decays, hereafter labelled τ_ℓ (τ_h), the response function is the distribution of the daughter lepton (jet) p_T as a fraction of the parent τ lepton p_T. To predict the contribution to the $\not{E}_T$ spectrum, the observed lepton in the control sample is replaced by a lepton (or jet), with the transverse momentum sampled from the appropriate response function; the difference between the sampled and original p_T is added vectorially to the $\not{E}_T$. This procedure is used to

Table 1
Observed yields in data and SM background predictions with their statistical and systematic uncertainties from the LS and MT methods. For the MT method the low $\not{E}_T$ (150–250 GeV) and low H_T (400–750 GeV) regions in the $N_b = 2$ sample are used as control regions and are not shown in the table.

$H_T > 400$ GeV						$N_b \geq 3$				
						Obs.		Pred.	± stat.	± syst.
$150 < \not{E}_T < 250$ GeV						94	MT	92	±5	±14
$250 < \not{E}_T < 350$ GeV						16	MT	14.5	±1.3	±2.5
$350 < \not{E}_T < 450$ GeV						2	MT	2.6	±0.4	±0.7
$\not{E}_T > 450$ GeV						0	MT	0.8	±0.2	±0.4
$H_T > 500$ GeV	$N_b = 2$					$N_b \geq 3$				
	Obs.		Pred.	± stat.	± syst.	Obs.		Pred.	± stat.	± syst.
$150 < \not{E}_T < 250$ GeV	350	LS	320	±16	±14	84	LS	71.1	±3.5	±8.3
$250 < \not{E}_T < 350$ GeV	55	LS	58.1	±7.2	±5.3	16	LS	12.4	±1.6	±1.8
$350 < \not{E}_T < 450$ GeV	10	LS	15.4	±4.3	±3.1	2	LS	3.1	±0.9	±0.7
$\not{E}_T > 450$ GeV	1	LS	0.7	$^{+2.3}_{-0.3}$	$^{+2.0}_{-0.2}$	0	LS	0.1	$^{+0.5}_{-0.0}$	$^{+0.4}_{-0.0}$
$H_T > 750$ GeV	$N_b = 2$					$N_b \geq 3$				
	Obs.		Pred.	± stat.	± syst.	Obs.		Pred.	± stat.	± syst.
$150 < \not{E}_T < 250$ GeV	141	LS	114.8	±9.4	±6.9	37	LS	25.9	±2.1	±3.1
							MT	31.8	±2.7	±4.8
$250 < \not{E}_T < 350$ GeV	26	LS	26.3	±4.9	±2.9	12	LS	5.9	±1.1	±1.0
		MT	37.9	±4.0	±3.5		MT	8.5	±0.9	±1.6
$350 < \not{E}_T < 450$ GeV	9	LS	10.6	$^{+3.8}_{-3.7}$	±2.4	2	LS	2.1	±0.7	±0.5
		MT	9.4	±1.4	±2.7		MT	1.9	±0.3	± 0.6
$\not{E}_T > 450$ GeV	1	LS	0.6	$^{+3.0}_{-0.2}$	$^{+1.9}_{-0.2}$	0	LS	0.1	$^{+0.7}_{-0.0}$	$^{+0.4}_{-0.0}$
		MT	3.1	±0.7	±1.5		MT	0.7	±0.2	± 0.4
$H_T > 1000$ GeV	$N_b = 2$					$N_b \geq 3$				
	Obs.		Pred.	± stat.	± syst.	Obs.		Pred.	± stat.	± syst.
$150 < \not{E}_T < 250$ GeV	46	LS	43.2	±6.1	±3.7	14	LS	10.4	±1.5	±1.5
		MT					MT	11.1	±1.6	±1.8
$250 < \not{E}_T < 350$ GeV	11	LS	9.9	±3.1	±1.7	4	LS	2.4	±0.7	±0.5
		MT	15.1	±2.5	±1.9		MT	3.6	±0.6	±0.8
$350 < \not{E}_T < 450$ GeV	4	LS	2.2	$^{+2.3}_{-1.6}$	$^{+2.2}_{-0.7}$	1	LS	0.4	$^{+0.5}_{-0.3}$	$^{+0.4}_{-0.2}$
		MT	4.7	±0.9	±1.5		MT	0.9	±0.2	± 0.4
$\not{E}_T > 450$ GeV	1	LS	0.1	$^{+2.2}_{-0.1}$	$^{+3.5}_{-0.1}$	0	LS	0.0	$^{+0.4}_{-0.0}$	$^{+0.7}_{-0.0}$
		MT	2.0	±0.5	±1.1		MT	0.5	±0.1	± 0.3

predict three background categories: single τ_ℓ, $\ell + \tau_h$, and $\ell + \tau_\ell$ events; the notation ℓ includes τ_ℓ components.

The $\not{E}_T$ spectrum obtained from applying the response functions to the control samples is corrected as a function of $\not{E}_T$ and H_T for branching fractions and efficiencies determined from MC simulation. These correction factors are roughly 0.2, 0.9, and 0.6 for the single τ_ℓ, $\ell + \tau_\ell$, and $\ell + \tau_h$ backgrounds, respectively, in all H_T bins. A correction is derived from simulation to account for a possible dependence on $\not{E}_T$ of the event selection and acceptance (note that this correction is consistent with one within the uncertainties).

SM backgrounds also arise from dilepton events. There are two categories of these events: those with both leptons reconstructed but where only one of the leptons is selected, and those with one lepton that is not reconstructed, which can occur either because of a reconstruction inefficiency or because the lepton lies outside the η acceptance of the detector. The estimate of the background from these processes is given by the simulated $\not{E}_T$ distribution, corrected by the ratio of the number of data to MC events in a dilepton control sample. This sample is the same as that used in the $\ell + \tau_\ell$ background prediction, but with an additional requirement of $\not{E}_T > 100$ GeV used to retain high trigger efficiency. Systematic uncertainties for the dilepton background estimate arise from the uncertainty in the data/MC scale factor, pileup, trigger and selection efficiencies, and the top-quark p_T spectrum.

The background composition is similar in each of the LS signal regions. For example, the signal region with $H_T > 500$ GeV, $N_b = 2$, and $350 < \not{E}_T < 450$ GeV has predicted single-lepton and single-τ backgrounds of 11.6 ± 5.2 and 1.8 ± 0.7, respectively. The

remainder of the background prediction, consisting of $\ell + \tau_h$, $\ell + \tau_\ell$, and dilepton events, is 2.0 ± 1.1. The total yields for all signal regions are given in Table 1 and Fig. 1 shows the $\not{E}_T$ distributions.

3.3. The missing transverse momentum model in the MT method

For values of $\not{E}_T$ well above the W boson mass, the SM $\not{E}_T$ distribution primarily arises from neutrino emission (genuine $\not{E}_T$) and has an approximately exponential shape. According to simulation, this distribution depends on H_T and, to a lesser extent, N_j and N_b, with only a small variation predicted for the non-exponential tails. Empirically, we find that the genuine $\not{E}_T$ distribution from $t\bar{t}$ events (the leading background term) can be parametrized well with the Pareto distribution [41], which is widely used in extreme value theory:

$$f_P(x; x_{\min}, \alpha, \beta) = \frac{1}{\alpha}\left(1 + \frac{\beta(x - x_{\min})}{\alpha}\right)^{-\frac{1}{\beta}-1}, \quad (1)$$

where $x_{\min}$, α, and β are the position, scale, and shape parameters, respectively. Eq. (1) yields an exponential function for $\beta = 0$. We set $x_{\min} = 150$ GeV, representing the lower bound of the $\not{E}_T$ spectrum to be described, while α and β are determined from a fit to data.

Both the control regions used for a fit of the $\not{E}_T$ model to data and the signal regions have selection criteria applied to H_T. Because of the correlation between the momentum of the leptonically decaying W boson and the momenta of the jets balancing it, restrictions on H_T affect the $\not{E}_T$ spectrum. We describe the ratio between the $\not{E}_T$ spectrum after imposing a lower bound
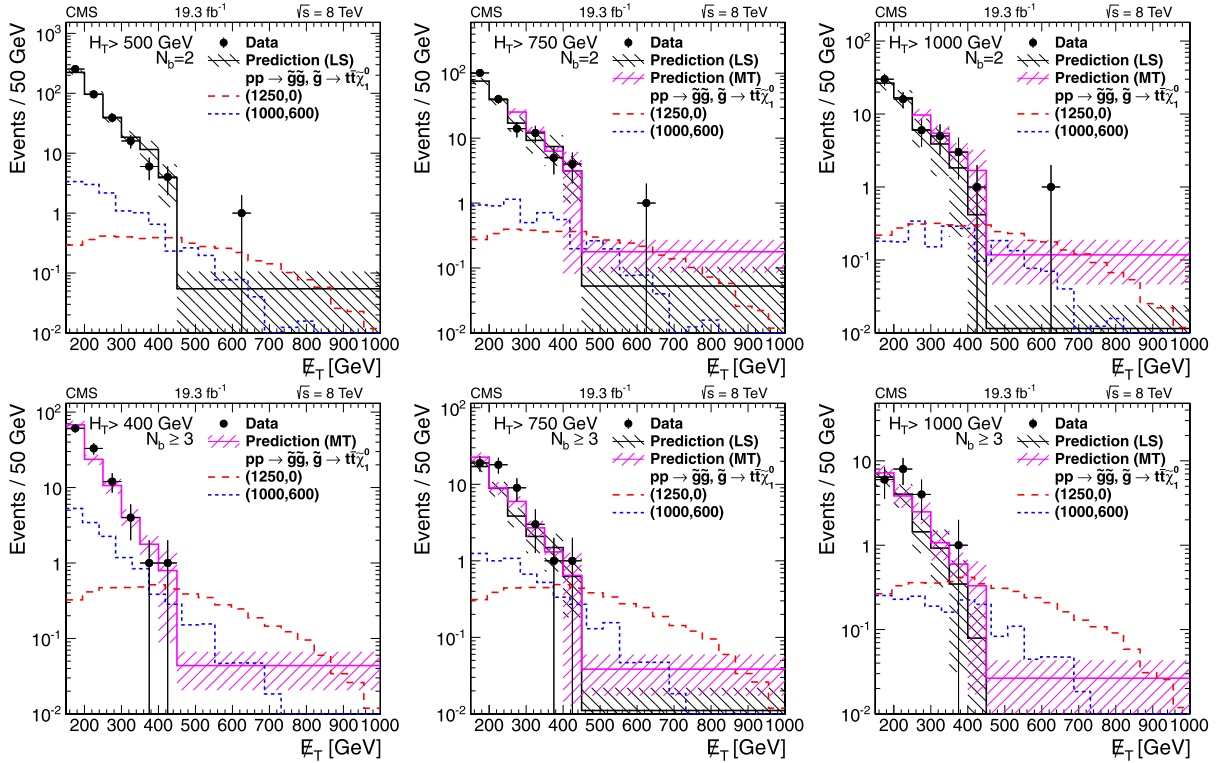
Fig. 1. Observed $\not{E}_T$ distributions and the corresponding predictions from the LS and MT methods for the $N_b = 2$ (top) and ≥ 3 (bottom) bins. The hatched areas show the combined statistical and systematic uncertainties of the predictions. For purposes of comparison, the distributions for SUSY model A with either $m_{\tilde{g}} = 1250$ GeV and $m_{\tilde{\chi}_1^0} = 0$ GeV, or $m_{\tilde{g}} = 1000$ GeV and $m_{\tilde{\chi}_1^0} = 600$ GeV, are shown. Values and uncertainties for the prediction in the highest $\not{E}_T$ bin correspond to the average for the range 450–1000 GeV.

on H_T and the inclusive $\not{E}_T$ spectrum by a generalized error function (corresponding to a skewed Gaussian distribution), similar to the approach described in Ref. [13]. The evolutions with H_T of the location and variance parameters of this function are determined from simulation and found to be linear. The results in simulation are found to be consistent with the dependence measured from a $t\bar{t}$-dominated control sample in data, defined by $N_j \geq 4$, $N_b \geq 2$, and $H_T > 400$ GeV. Systematic uncertainties related to the error functions are determined from this comparison and from the difference between linear and quadratic models of the function parameters. The $\not{E}_T$ spectrum in exclusive bins of N_b is also affected by an acceptance effect due to the p_T requirement on the b-tagged jets: in $t\bar{t}$ events at low H_T, high values of $\not{E}_T$ correspond to low values of the p_T of the b quark associated with the leptonically decaying W boson and tend to move events to lower b-jet multiplicities. We therefore apply an acceptance correction when applying the $\not{E}_T$ model to events with one or two b-tagged jets. For $N_b = 2$ and $150 < \not{E}_T < 1000$ GeV, the size of the correction is 12% for $H_T = 750$ GeV and is smaller for larger H_T.

The b-jet multiplicity distribution is used to estimate the ratio of the $W + \text{jets}$ background to the $t\bar{t}$ background as a function of H_T. The H_T distribution of $t\bar{t}$ events is extracted from the $N_b = 2$ sample as described in Ref. [13]. The contribution of $W + \text{jets}$ events for $\not{E}_T > 150$ GeV is approximately 1%. Uncertainties related to other non-leading background components are estimated by varying the corresponding cross sections and are found to be small. Based on the measured ratio of $W + \text{jets}$ to $t\bar{t}$ background events, the Pareto distribution describing the leading background term is combined with the shape of the $W + \text{jets}$ $\not{E}_T$ distribution from simulation to form the full model describing the genuine $\not{E}_T$ distribution of SM events.

3.4. The fit to the missing transverse momentum spectrum in the MT method

The model for genuine $\not{E}_T$ in SM events is convolved with the $\not{E}_T$ resolution templates described in Section 3.1 and used in a simultaneous fit to the $\not{E}_T$ shapes in control regions in the $N_b = 1$ and $N_b = 2$ bins. The control regions are chosen in order to ensure reasonably small statistical uncertainties and to limit potential contributions from signal events: for events with two b-tagged jets the control region is defined by $400 < H_T < 750$ GeV and $150 < \not{E}_T < 400$ GeV, while for one b-tagged jet it is extended to $400 < H_T < 2500$ GeV and $150 < \not{E}_T < 1500$ GeV.

Because of limited statistical precision in the control regions, we are unable to obtain a reliable estimate of β from data. We use a constraint from simulation together with an uncertainty derived from a comparison between data and simulation in control regions with lower jet multiplicity. The constraint is implemented as a Gaussian term corresponding to the value and its statistical uncertainty obtained from simulation, $\beta = 0.03 \pm 0.01$. The prediction from simulation for $N_j = 3$–5 is $\beta = 0.15$–0.05, consistent with the data. The maximum difference between data and simulation in any of these three N_j bins of 0.05 is used to define a systematic uncertainty in the prediction. The parameters of the error function (Section 3.3) are constrained by Gaussian terms reflecting the respective values and covariance from simulation.

The predictions for the $N_b = 2$ signal regions are obtained by integrating the function representing the $\not{E}_T$ model over the relevant $\not{E}_T$ range and summing over the H_T bins. In each H_T bin, the predicted distribution is scaled to match the observed number of events in the normalization region defined by $150 < \not{E}_T < 250$ GeV. The statistical uncertainties of the predictions are evaluated by repeating the procedure using parameter values randomly generated

according to the results of the fit, including the covariance matrix. The predictions are stable to within 1% if the $\not{E}_T$ model described in Ref. [13] is used in place of the model described here.

The results of the MT method can be affected by several systematic uncertainties that are related to detector effects, assumptions made on the shape of the distribution, as well as theoretical uncertainties and the contamination due to non-leading backgrounds. Systematic uncertainties related to the jet and $\not{E}_T$ scale, lepton reconstruction efficiencies, W-boson polarization in $t\bar{t}$ events, and cross sections of non-leading backgrounds are evaluated in the same way as for the LS method (Section 3.1). Effects due to b-jet identification efficiencies and pileup are also taken into account. In addition, the following uncertainties specific to the MT method are considered. The β parameter and parameters of the error function are varied as described above. The differences with respect to the standard result define the systematic uncertainty for each signal region. The effects of a possible residual non-linearity in the error function parameters versus H_T are also taken into account. To test the validity of the method, the procedure is applied to simulated events. The resulting background predictions are found to be statistically consistent with the true numbers from simulation. Conservatively, the maximum of the relative difference and its uncertainty are assigned as a further systematic uncertainty ("closure"). The dominant contributions to the systematic uncertainty are related to the $\not{E}_T$ model (1–35%, depending on the H_T and $\not{E}_T$ bin) and the closure (8–43%). Uncertainties related to the theoretical predictions of the cross section for SM backgrounds, the jet and $\not{E}_T$ scale, and pileup contribute each with less than 5%.

3.5. Background estimation in the $N_b \geq 3$ bin

The numbers of data events in the $N_b \geq 3$ control samples are too low for an application of the LS or MT technique. Therefore we estimate the background for high b-jet multiplicities by applying to the background predictions for $N_b = 2$ transfer factors (R_{32}) that give the ratio of the number of events with ≥ 3 and $= 2$ b-tagged jets for each of the signal regions. The central values for the R_{32} factors are determined from simulation. The scale factors R_{32} increase with jet multiplicity from approximately 0.05 for events with three jets to approximately 0.2 in events with ≥ 6 jets because of the higher probability of misidentifying one or more jets. For constant jet multiplicity they do not demonstrate a strong dependence on H_T.

The ratios between $N_b \geq 3$ and $= 2$ events in data and simulation could differ because of incorrect modeling of the heavy-flavor content, the jet kinematics, and uncertainties in the b-tagged jet misidentification rates. To probe the impact of the first source of uncertainties, the weight of events with at least one c quark is varied by ±50%. A variation of the same size is applied to events with additional b- or c-quark pairs. The effect of possible differences between data and simulation in the kinematics of the system of non-b jets on R_{32} is tested in a control sample with exactly two b-tagged jets. The remaining jets in the event are randomly assigned a parton flavor: one jet is marked as a c-quark jet, while the others are marked as light-quark jets. Based on this assignment the ratio of probabilities to tag at least one additional jet is calculated. This procedure is applied to both data and simulation. Good agreement is found and the residual difference is interpreted as a systematic uncertainty. The uncertainty related to b-tagged jet misidentification is evaluated from the uncertainties of the misidentification scale factors relative to simulation. The total systematic uncertainties for R_{32} are approximately 9–19% depending on the signal region. An additional verification is performed in two control regions at higher lepton p_T (>30 GeV), lower H_T (<400 GeV) and $\not{E}_T$ ($150 < \not{E}_T < 250$ GeV), and $N_j = 5$ or ≥ 6. In

both regions the values of R_{32} obtained in simulation are compatible with the ones observed in data.

In the LS method, the transfer factors are applied to the signal regions for $H_T > 500$, 750, and 1000 GeV. In the MT method, signal regions for $H_T > 400$ GeV and $150 < \not{E}_T < 250$ GeV are added for the $N_b \geq 3$ bin, corresponding to the limits of the control and normalization regions in the $N_b = 2$ bin, respectively.

3.6. Results for signal regions in missing transverse momentum and H_T bins

The predictions of both methods are compared with the observed number of events in Table 1. For the LS method the predictions consist of the single-lepton and τ-lepton backgrounds with a small contribution from dilepton events. Drell–Yan events are heavily suppressed by the N_j, N_b, and kinematic requirements. The yield of this small component of the background is taken from simulation. For the MT method the predictions consist of the inclusive estimation of the leading backgrounds. Additional contributions to the signal regions from multijet events are heavily suppressed, but their cross section is large and not precisely known. Therefore, they are predicted from data based on scaling the sideband of the relative lepton isolation distribution. These contributions are neglected as they are found to constitute 1% or less of the total background in all cases.

The corresponding observed and predicted $\not{E}_T$ spectra are shown in Fig. 1 for the two b-jet multiplicity bins and different H_T requirements. The two methods differ in their leading systematic terms and in the correlations they exhibit between the background predictions in different signal regions. The predictions are consistent, an indication of the robustness of the methods. No excess is observed in the tails of the $\not{E}_T$ distributions with respect to the expectations from SM processes. The results are interpreted in terms of upper limits on the production cross section for different benchmark models in Section 5.

4. Search using S_T^{lep} and $\Delta\phi(W, \ell)$

After applying the selection criteria in Section 2, the sample is dominated by single-lepton $t\bar{t}$ events. In the *delta phi* ($\Delta\phi$) analysis method, this background is further reduced by applying a requirement on the azimuthal angle between the W-boson candidate and the charged lepton. The W-boson candidate transverse momentum is obtained as the vector sum of the lepton p_T and the $\not{E}_T$ vectors. For single-lepton $t\bar{t}$ events, the angle between the W-boson direction and the charged lepton has a maximum value, which is fixed by the mass of the W boson and its momentum. Furthermore, the requirement (direct or indirect) of large $\not{E}_T$ selects events in which the W boson yielding the lepton and the neutrino is boosted, thus resulting in a fairly narrow distribution in $\Delta\phi(W, \ell)$. On the other hand, in SUSY decays, the "effective W boson" that is formed from the vector sum of the transverse momenta of the charged lepton and the $\not{E}_T$ vector will have no such maximum. Since the $\not{E}_T$ results mostly from two neutralinos, the directions of which are largely independent of the lepton flight direction, the $\Delta\phi(W, \ell)$ distribution is expected to be flat.

Distributions of $\Delta\phi(W, \ell)$ in different S_T^{lep} bins are shown for the $N_b \geq 3$ and $N_j \geq 6$ samples in Fig. 2. We select $\Delta\phi(W, \ell) > 1$ as the signal region. The complementary sample, events with $\Delta\phi(W, \ell) < 1$, constitutes the control region. It can be seen that this selection is effective in reducing the background from single-lepton $t\bar{t}$ decays; the dominant background in the signal regions comes from dilepton $t\bar{t}$ events. Table 2 shows the event yields from simulation for the signal and control regions in different S_T^{lep} bins for events with $N_b \geq 3$, which have the highest sensitivity to the
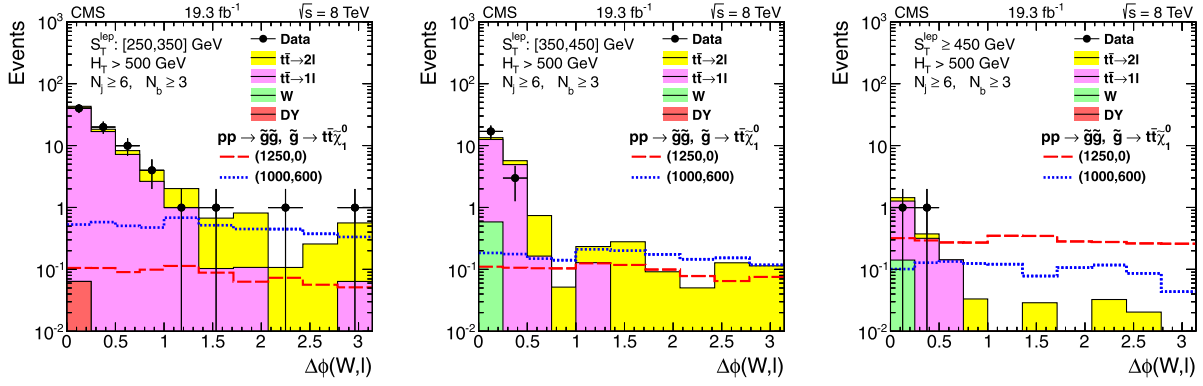
Fig. 2. The $\Delta\phi(W, \ell)$ distribution in simulation and data for the combined e and μ channels with $N_b \geq 3$ and $N_j \geq 6$. The SM simulation is normalized to the data in the control region ($\Delta\phi(W, \ell) < 1$). The simulated SM yields in the signal region ($\Delta\phi(W, \ell) > 1$) are shown only for illustration, as the actual estimate is obtained with the procedure described in the text. The distributions expected for signal are illustrated using two mass points from model A, with masses specified as $(m_{\tilde{g}}, m_{\tilde{\chi}_1^0})$ in GeV. Left: $250 < S_T^{lep} < 350$ GeV, center: $350 < S_T^{lep} < 450$ GeV, and right: $S_T^{lep} > 450$ GeV.

Table 2
Event yields for the combined e and μ channels, as predicted by simulation, for $N_j \geq 6$ and $N_b \geq 3$. The R_{CS} column lists the ratio of yields in the signal and control regions. The yields for signal benchmark points are shown for comparison, with the $(\tilde{g}, \tilde{\chi}_1^0)$ masses (in GeV) listed in brackets. The uncertainties are statistical only.

| Sample	$250 < S_T^{lep} < 350$ GeV			$350 < S_T^{lep} < 450$ GeV			$S_T^{lep} > 450$ GeV		
	Signal	Control	R_{CS}	Signal	Control	R_{CS}	Signal	Control	R_{CS}
$t\bar{t}(1\ell)$	0.8 ± 0.2	43.2 ± 1.8	0.02	0.1 ± 0.1	11.6 ± 1.0	0.01	<0.01	3.4 ± 0.5	n/a
$t\bar{t}(\ell\ell)$	2.0 ± 0.3	4.0 ± 0.4	0.51	0.5 ± 0.1	1.6 ± 0.3	0.34	0.2 ± 0.1	0.6 ± 0.2	0.35
W	<0.23	<0.23	n/a	<0.24	0.4 ± 0.4	n/a	<0.22	0.3 ± 0.3	n/a
DY	<0.03	<0.03	n/a	<0.02	<0.02	n/a	<0.03	<0.03	n/a
Multijet	<0.05	<0.05	n/a	<0.01	<0.01	n/a	<0.01	<0.01	n/a
Single t	0.4 ± 0.2	1.9 ± 0.3	0.21	<0.08	0.8 ± 0.2	n/a	<0.08	0.4 ± 0.2	0.04
SM all	3.3 ± 0.4	49.0 ± 1.8	0.07	0.6 ± 0.2	14.4 ± 1.1	0.04	0.2 ± 0.1	4.7 ± 0.7	0.05
Model A	Signal	Control	R_{CS}	Signal	Control	R_{CS}	Signal	Control	R_{CS}
(1000, 600)	2.80 ± 0.10	2.09 ± 0.09	1.34	1.00 ± 0.06	0.65 ± 0.05	1.54	0.55 ± 0.05	0.49 ± 0.04	1.13
(1250, 0)	0.45 ± 0.01	0.40 ± 0.01	1.12	0.56 ± 0.02	0.42 ± 0.01	1.32	1.78 ± 0.03	1.16 ± 0.02	1.54
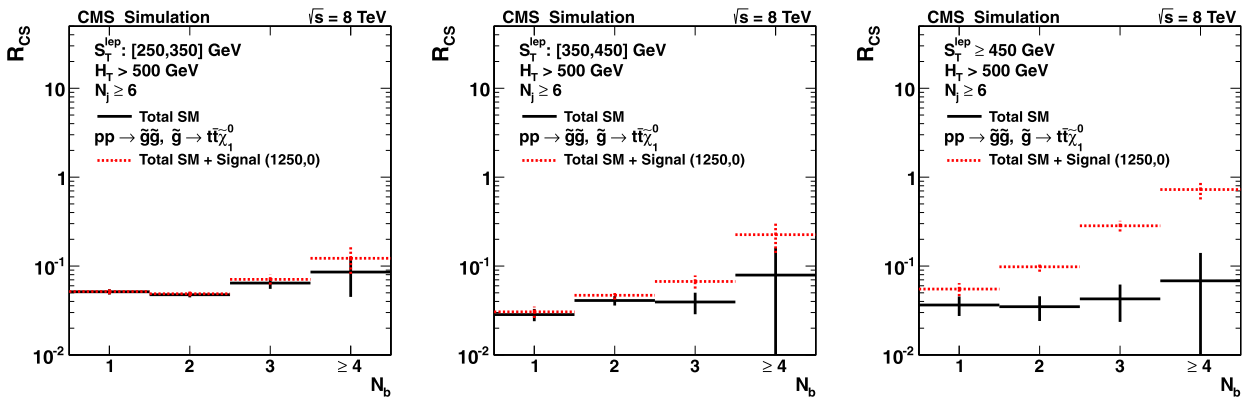
Fig. 3. The transfer factor R_{CS} in simulation for the combined e and μ channels as a function of N_b for events with $N_j \geq 6$. The lines correspond to SM only and to the sum of SM backgrounds and signal corresponding to the mass point ($m_{\tilde{g}} = 1250$ GeV, $m_{\tilde{t}} = 0$ GeV) of model A. Left: $250 < S_T^{lep} < 350$ GeV, center: $350 < S_T^{lep} < 450$ GeV, and right: $S_T^{lep} > 450$ GeV.

SUSY signal. The contributions from $t\bar{t}Z$, $t\bar{t}W$, $t\bar{t}H$, and diboson events are insignificant and have not been used for the results shown in this section. The search also uses events with $N_b = 2$, albeit with smaller sensitivity.

4.1. Prediction of standard model background

The estimate of the SM background in the signal region is obtained using the data and some input from simulation. We define a transfer factor, R_{CS}, as the ratio of the number of events with $\Delta\phi(W, \ell) > 1$ to the number with $\Delta\phi(W, \ell) < 1$. Fig. 3 displays the value of R_{CS} as a function of N_b for the SM alone and also with the addition of signal from a SUSY benchmark scenario. In the absence of a SUSY signal, the value of R_{CS} is roughly independent of the b-jet multiplicity. In the presence of a signal containing four top quarks, however, the value of R_{CS} in the $N_b \geq 2$ bins changes significantly, whereas it remains unchanged in the $N_b = 1$ bin, which is dominated by background from SM processes.

Table 3

Data yields and the corresponding R_{CS} values for events with $N_j \geq 6$ and $N_b = 1$.

		S_T^{lep} [GeV]	Control	Signal	R_{CS}
$N_b = 1$	e	[250, 350]	169	6	0.04 ± 0.01
		[350, 450]	44	3	0.07 ± 0.04
		>450	17	0	<0.06
	μ	[250, 350]	192	9	0.05 ± 0.02
		[350, 450]	55	2	0.04 ± 0.03
		>450	10	0	<0.1

Table 4

Comparison of the simulated yields, combined for the e and μ channels, in the signal region and the estimate using R_{CS} from the $N_b = 1$ sample. The κ_{CS} factor is calculated as the ratio of the true yield in the signal region ("MC truth") and the predicted number.

	S_T^{lep} [GeV]	Predicted (without κ_{CS})	MC truth	κ_{CS}
$N_b = 2$	[250, 350]	15.26 ± 1.06	14.17 ± 0.91	0.93 ± 0.09
	[350, 450]	2.10 ± 0.35	3.04 ± 0.35	1.45 ± 0.29
	>450	0.90 ± 0.23	0.87 ± 0.26	0.97 ± 0.39
$N_b \geq 3$	[250, 350]	2.59 ± 0.21	3.34 ± 0.44	1.29 ± 0.20
	[350, 450]	0.44 ± 0.08	0.64 ± 0.17	1.45 ± 0.47
	>450	0.18 ± 0.06	0.22 ± 0.09	1.22 ± 0.61

Given this observation, we obtain the transfer factors used to predict the SM background for different values of N_b, $R_{CS}^{pred}(N_b)$, as $R_{CS}^{pred}(N_b) = R_{CS}(N_b = 1) \cdot \kappa_{CS}(N_b)$, where $R_{CS}(N_b = 1)$ is the R_{CS} factor measured in data with $N_b = 1$ (Table 3) and κ_{CS} is a correction factor obtained from simulation (Table 4), introduced to account for any residual dependence of R_{CS} on N_b. The transfer factors $R_{CS}^{pred}(N_b)$ are calculated independently for each bin in S_T^{lep}.

The calculation of the κ_{CS} factor in simulation is shown in Table 4, which lists the yield without a κ_{CS} factor correction, and the observed event yields, as well as the corresponding κ_{CS} correction factors for $N_b \geq 3$. The κ_{CS} factor ranges from 0.93 to 1.45 with statistical uncertainties up to ± 0.6. The large statistical uncertainty reflects the very small event yields expected in the signal region from SM processes.

We observe only a weak dependence of the transfer factor R_{CS} on N_j and, as stated above, on N_b. Two sources of this dependence have been identified: the relative composition of SM samples (W + jets, $t\bar{t}(1\ell)$, $t\bar{t}(\ell\ell)$, single top quark), and the residual dependence of R_{CS} within each SM sample. The effect of each source on R_{CS} is found to be <50%. The application of the κ_{CS} factor compensates for these effects and incorporates their uncertainties. A potential signal would result in much larger values of R_{CS} (e.g., of up to a factor of five larger for the benchmark points) than the variations above, as can be seen from Fig. 3.

The only elements of the background estimate that depend on simulation are the κ_{CS} factors. Most potential sources of systematic uncertainties leave κ_{CS} unaffected, since the correction factor reflects only residual changes in the value of R_{CS} from $N_b = 1$ to $N_b \geq 3$ ($N_b = 2$) as a result of each systematic uncertainty. Systematic uncertainties are estimated as in Section 3, i.e. by calculating the change induced in the scale factor, κ_{CS}, from various effects and propagating this change to the predicted yields. The jet/$\not{E}_T$ energy scale and the b-tagging efficiencies are varied within their uncertainties. For each independent source (energy scale, heavy- and light-parton tagging efficiencies) the effects of the upwards and downwards variations are averaged. The W + jets cross section is varied by 30% as in Ref. [12]. The cross section for W + b$\bar{b}$ is varied by 100% [42,43] and that for single-top-quark production by 50% [44]. We assign an uncertainty of 5 and 10%, respectively,

to the W boson and $t\bar{t}$ polarizations [45,40]. These effects are negligible.

Since the estimate of the background in the signal region is based on ratios of events in the data and the κ_{CS} factor that only depends on the number of b-tagged jets, the systematic uncertainties of the background prediction are expected to be the same for the electron and muon samples. This is confirmed with an explicit calculation of these uncertainties, and thus the final result uses the combination of the uncertainties from the two lepton flavors. The overall systematic uncertainty found for κ_{CS}, which is dominated by the limited statistics in the simulated samples, is 23%, 45% and 70%, respectively, in the three S_T^{lep} ranges. The total systematic uncertainty of the background prediction is dominated by the statistical uncertainty that arises due to the limited number of events in the data control samples.

4.2. Multijet background estimate

Contributions of multijet events to the control and signal regions could affect the correction factors. Therefore we estimate these contributions from data. For the muon channel, the MC prediction for the multijet background is smaller than all other backgrounds by two to three orders of magnitude. This was confirmed by an estimate from data in the previous single-lepton SUSY search [12].

In the electron channel, the multijet background is larger than in the muon channel, but it remains significantly smaller than the other backgrounds. We make use of the method described in Ref. [45], employing a control sample in data that is enriched in electrons from multijet events, obtained by inverting some of the electron identification requirements ("antiselected" sample). While the method works well at low N_b and N_j, it yields statistically limited results in the samples with higher N_b and higher N_j. To obtain more precise predictions for the multijet background in these regions, the estimate from the $N_b = 1$ sample is extrapolated with two methods that rely on the relative insensitivity of the multijet background to N_b. The results of these methods are found to be consistent, and the fraction of multijet events is determined to be less than 5–7% of the total number of data events observed in the control region. Based on the antiselected sample, the corresponding transfer factor for multijet events is estimated to be smaller than approximately 2%. The multijet contamination in the signal region ($\Delta\phi(W, \ell) > 1$) is therefore determined to be negligible and so the multijet background is subtracted only in the control region.

4.3. Results for signal regions in S_T^{lep} and N_b

The background prediction method is validated with the $3 \leq N_j \leq 5$ control sample, which is background dominated with dilepton $t\bar{t}$ events and with a relative contribution from W + jets larger than in the signal region. The compatibility between the predicted and observed yields in this sample is demonstrated by the results shown in the left portion of Table 5.

The predicted and observed data yields in the signal regions are also presented in Table 5. In the single case of a control region with zero observed events the uncertainty is estimated assuming that one event was present. Combining all signal bins we predict 19.2 ± 4.0 events and observe 26. In the $N_b \geq 3$ bins, which are the most relevant regions for the signal, we predict 5.3 ± 1.5 events and observe 4. For $S_T^{lep} > 350$ GeV we predict 5.6 ± 2.5 events and observe 4.

5. Interpretation

The compatibility between the observed and predicted event counts in the searches described above is used to exclude regions

Table 5

Event yields in data for the $3 \leq N_j \leq 5$ (validation) and $N_j \geq 6$ (signal) samples. The number of events in the control regions used for the predictions are also shown. For the lower jet multiplicity validation test, only the statistical uncertainties stemming from the event counts in the control regions are given, while statistical and systematic uncertainties are listed for the signal region prediction.

		S_T^{lep} [GeV]	$3 \leq N_j \leq 5$			$N_j \geq 6$		
			Control	Pred.	Obs.	Control	Pred.	Obs.
$N_b = 2$	e	[250, 350]	548	34.2 ± 5.4	30	112	$3.8 \pm 1.8 \pm 0.6$	9
		[350, 450]	174	5.1 ± 1.9	8	28	$2.7 \pm 1.9 \pm 0.8$	2
		>450	61	5.6 ± 2.1	1	9	$0.0 \pm 0.4 \pm 0.2$	0
	μ	[250, 350]	632	41.9 ± 5.6	59	141	$6.0 \pm 2.2 \pm 0.9$	9
		[350, 450]	188	8.5 ± 2.4	11	24	$1.4 \pm 1.1 \pm 0.4$	2
		>450	71	2.5 ± 1.3	1	9	$0.0 \pm 0.7 \pm 0.2$	0
$N_b \geq 3$	e	[250, 350]	70	3.9 ± 0.9	2	45	$1.9 \pm 0.9 \pm 0.4$	4
		[350, 450]	12	0.3 ± 0.2	2	7	$0.9 \pm 0.7 \pm 0.4$	0
		>450	4	0.3 ± 0.2	0	0	$0.0 \pm 0.1 \pm 0.03$	0
	μ	[250, 350]	59	3.9 ± 0.8	5	28	$1.9 \pm 0.8 \pm 0.4$	0
		[350, 450]	25	1.1 ± 0.4	0	13	$0.6 \pm 0.5 \pm 0.3$	0
		>450	7	0.3 ± 0.2	0	2	$0.0 \pm 0.2 \pm 0.1$	0

in the parameter space of the three models of gluino-mediated production of final states with four top quarks and two LSPs introduced in Section 2. The expected signal yield obtained from simulation is corrected for small differences in the efficiencies between data and simulation and for an overestimation of events with high-p_T radiated jets in MadGraph, as described in Ref. [11]. Systematic uncertainties in the signal yield due to uncertainty in the jet/$\not{E}_T$ scale [36], initial-state radiation, PDFs [46], pileup, b-tagging scale factors [37], lepton efficiency, and trigger efficiency are calculated for each of the models and for every mass combination. The uncertainty due to the measurement of the integrated luminosity is 2.6% [47]. For model A, the total uncertainty in the signal yields ranges from 20% to 60%. The largest uncertainties are related to the PDFs and occur in regions with small mass differences $m_{\tilde{g}} - m_{\tilde{\chi}_1^0}$ and high $m_{\tilde{g}}$.

The modified-frequentist CL$_S$ method [48–50] with a one-sided profile likelihood ratio test statistic is used to define 95% confidence level (CL) upper limits on the production cross section for each model and mass combination. Statistical uncertainties related to the observed number of events in control regions are modeled as Poisson distributions. All other uncertainties are assumed to be multiplicative and are modeled with lognormal distributions.

For each method, several of the signal regions defined in Sections 3 and 4 are used simultaneously. In the LS method, three different sets of signal regions are defined, with a lower H_T bound of either 500, 750, or 1000 GeV. For each model point, the signal region set with the most stringent expected sensitivity is chosen and the six ($\not{E}_T$, N_b) bins with $\not{E}_T > 250$ GeV are used simultaneously. The most stringent limits are typically obtained for the lowest H_T threshold. In the MT method, the requirement $H_T > 750$ GeV globally yields the best results when combined with the region $400 < H_T < 750$ GeV in the $N_b \geq 3$ bin. The samples in the two b-jet multiplicity bins are further divided into $\not{E}_T$ bins with lower bounds at 250, 350, and 450 GeV. For the $N_b \geq 3$ bin, a low $\not{E}_T$ region of 150–250 GeV is added, and the $\not{E}_T$ bins above 250 GeV are combined for $400 < H_T < 750$ GeV. In the $\Delta\phi(W, \ell)$ method all 12 signal regions defined by the three S_T^{lep} bins, the two b-jet multiplicity requirements, and the two lepton flavors are used simultaneously for all model points. For all three methods, correlations between the uncertainties in different signal regions and between signal yields and background predictions, are taken into account, as well as the effect of signal contamination on the predictions.

Upper limits on the cross section at a 95% CL are set in the parameter plane of the three models. Corresponding mass limits are derived with the next-to-leading order (NLO) + next-to-leading logarithm (NLL) gluino production cross section [51–55] as

a reference. The uncertainty on this cross section is determined as described in Ref. [56]. These limits are summarized in Fig. 4, which shows a comparison of the mass limits obtained for signal regions in H_T and $\not{E}_T$, cross section and mass limits for the signal regions in S_T^{lep} and $\Delta\phi(W, \ell)$, and a comparison of the observed mass limits obtained by the three methods. For each of the considered models the LS and MT methods show a similar reach; the most stringent limits are set by the $\Delta\phi$ method. For model A, with off-shell top squarks, the limits extend to a gluino mass of 1.26 TeV for the lowest LSP masses and to an LSP mass of 580 GeV for $m_{\tilde{g}} = 1.1$ TeV. At low gluino masses the sensitivity extends to the region $m_{\tilde{\chi}_1^0} > m_{\tilde{g}} - 2m_t$. For model B, where the top squarks are on-shell, the limits for $m_{\tilde{\chi}_1^0}$ reach 560 GeV for $m_{\tilde{t}} = 800$ GeV. For model C the gluino mass limits for low LSP mass are similar to model A for $m_{\tilde{t}} > 500$ GeV but decrease to $m_{\tilde{g}} = 1.0$ TeV for lower stop masses because the signal populates the lower $\not{E}_T$ region, which has higher background. For $m_{\tilde{g}} = 1.0$ TeV, the limits cover the full range of top-squark masses if the LSP mass lies below approximately 530 GeV. Conservatively, these limits are derived from the reference cross section minus one standard deviation [56].

6. Summary

A sample of proton–proton collisions recorded with the CMS detector at a center-of-mass energy of 8 TeV and corresponding to an integrated luminosity of 19.3 fb^{-1} has been used for a search for new physics in events with a single isolated electron or muon, multiple high-p_T jets, including identified b jets, and missing transverse momentum. This event topology is a possible signature for the production of supersymmetric particles in R-parity conserving models, in particular the production of gluinos with subsequent decays into top squarks. The dominant standard model background in a search region defined by the presence of at least six jets, including at least two jets identified as originating from the fragmentation of b quarks, is due to $t\bar{t}$ production.

The search is performed with two sets of signal regions, and uses three different methods, each based on data, to estimate the leading background contributions. The *lepton spectrum* and the *missing transverse momentum template* methods are designed as searches in the high H_T, high $\not{E}_T$ region. They estimate the SM backgrounds (dominated by single-lepton $t\bar{t}$ decays) for events with two identified b jets and extrapolate these predictions to additional signal regions requiring ≥3 b-tagged jets. The first of these methods uses the lepton p_T distribution to estimate the $\not{E}_T$ spectrum while the second obtains the predictions in a parametrized form by fitting a $\not{E}_T$ model to control regions in data. The *delta*
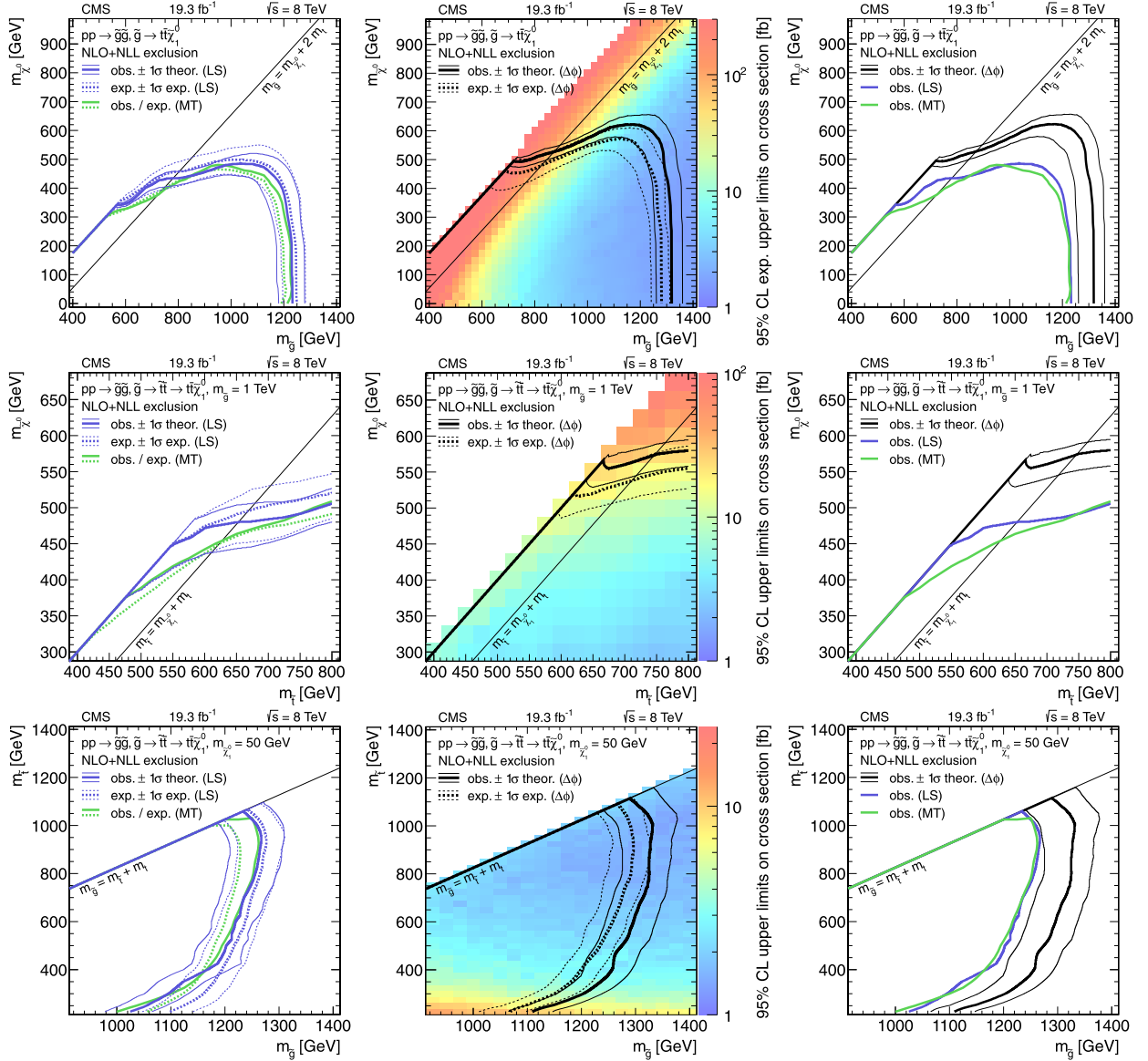
Fig. 4. Cross section and mass limits at 95% CL in the parameter planes of (top) model A, (center) model B, and (bottom) model C. The color shading indicates the observed limit on the cross section. The solid (dashed) lines show the observed (expected) mass limits, with the thick lines representing the central value and the thin lines the variations from the theoretical [56] (experimental) uncertainties. Left column: mass limits for signal regions in H_{T} and $\not{E}_{\mathrm{T}}$ (LS and MT) and uncertainty bands for the LS method (the uncertainties for the MT method have similar size). Central column: cross section and mass limits for signal regions in $S_{\mathrm{T}}^{\mathrm{lep}}$ and $\Delta\phi(W, \ell)$ ($\Delta\phi$). Right column: comparison of the observed mass limits for the three methods.

phi method uses the azimuthal angle between the lepton and W boson directions as a discriminating variable, leading to a strong suppression of the single-lepton backgrounds and leaving dilepton t$\bar{\mathrm{t}}$ events as the leading SM contribution. The signal regions are defined by the use of the same two b-jet multiplicity requirements and by bins in $S_{\mathrm{T}}^{\mathrm{lep}}$, which probes the total leptonic (ℓ and ν) scalar transverse momentum in the event. While the *delta phi* approach shows the highest sensitivity, the use of different methods, which probe complementary kinematic aspects and both hadronic and leptonic event characteristics, increases the robustness of this search. Together these methods examine the event sample in both high- and low-yield regions to provide sensitivity to signal topologies with high hadronic activity, missing transverse momentum, and at least two b jets.

No significant excess is observed in any of the signal regions. Upper limits are set at 95% CL on the product of production cross section and branching fraction for three benchmark models of gluino pair production with subsequent decay into virtual or on-shell top squarks, where each of the two top squarks decays in turn into a top quark and the lightest supersymmetric particle. In the case of decays via virtual top squarks and for light LSPs, gluino masses below 1.26 TeV are excluded.

Acknowledgements

References

[1] J. Wess, B. Zumino, Supergauge transformations in four-dimensions, Nucl. Phys. B 70 (1974) 39, http://dx.doi.org/10.1016/0550-3213(74)90355-1.

[2] S. Dimopoulos, H. Georgi, Softly broken supersymmetry and SU(5), Nucl. Phys. B 193 (1981) 150, http://dx.doi.org/10.1016/0550-3213(81)90522-8.

[3] H.P. Nilles, Supersymmetry, supergravity and particle physics, Phys. Rep. 110 (1984) 1, http://dx.doi.org/10.1016/0370-1573(84)90008-5.

[4] H.E. Haber, G.L. Kane, The search for supersymmetry: Probing physics beyond the standard model, Phys. Rep. 117 (1985) 75, http://dx.doi.org/10.1016/0370-1573(85)90051-1.

[5] R. Barbieri, S. Ferrara, C.A. Savoy, Gauge models with spontaneously broken local supersymmetry, Phys. Lett. B 119 (1982) 343, http://dx.doi.org/10.1016/0370-2693(82)90685-2.

[6] S. Dawson, E. Eichten, C. Quigg, Search for supersymmetric particles in hadron–hadron collisions, Phys. Rev. D 31 (1985) 1581, http://dx.doi.org/10.1103/PhysRevD.31.1581.

[7] N. Sakai, Naturalness in supersymmetric GUTS, Z. Phys. C 11 (1981) 153, http://dx.doi.org/10.1007/BF01573998.

[8] S. Dimopoulos, G.F. Giudice, Naturalness constraints in supersymmetric theories with nonuniversal soft terms, Phys. Lett. B 357 (1995) 573, http://dx.doi.org/10.1016/0370-2693(95)00961-J, arXiv:hep-ph/9507282.

[9] M. Papucci, J.T. Ruderman, A. Weiler, Natural SUSY endures, J. High Energy Phys. 09 (2012), http://dx.doi.org/10.1007/JHEP09(2012)035, 035, arXiv:1110.6926.

[10] C. Brust, A. Katz, S. Lawrence, R. Sundrum, SUSY, the third generation and the LHC, J. High Energy Phys. 03 (2012), http://dx.doi.org/10.1007/JHEP03(2012)103, 103, arXiv:1110.6670.

[11] CMS Collaboration, Search for top-squark pair production in the single-lepton final state in pp collisions at $\sqrt{s} = 8$ TeV, Eur. Phys. J. C 73 (2013), http://dx.doi.org/10.1140/epjc/s10052-013-2677-2, 2677, arXiv:1308.1586.

[12] CMS Collaboration, Search for supersymmetry in pp collisions at $\sqrt{s} = 7$ TeV in events with a single lepton, jets, and missing transverse momentum, Eur. Phys. J. C 73 (2013), http://dx.doi.org/10.1140/epjc/s10052-013-2404-z, 2404, arXiv:1212.6428.

[13] CMS Collaboration, Search for supersymmetry in final states with a single lepton, b-quark jets, and missing transverse energy in proton–proton collisions at $\sqrt{s} = 7$ TeV, Phys. Rev. D 87 (2013), http://dx.doi.org/10.1103/PhysRevD.87.052006, 052006, arXiv:1211.3143.

[14] ATLAS Collaboration, Multi-channel search for squarks and gluinos in $\sqrt{s} = 7$ TeV pp collisions with the ATLAS detector, Eur. Phys. J. C 73 (2013), http://dx.doi.org/10.1140/epjc/s10052-013-2362-5, 2362, arXiv:1212.6149.

[15] ATLAS Collaboration, Search for light top squark pair production in final states with leptons and b-jets with the ATLAS detector in $\sqrt{s} = 7$ TeV proton–proton collisions, Phys. Lett. B 720 (2013) 13, http://dx.doi.org/10.1016/j.physletb.2013.01.049, arXiv:1209.2102.

[16] ATLAS Collaboration, Further search for supersymmetry at $\sqrt{s} = 7$ TeV in final states with jets, missing transverse momentum and isolated leptons with the ATLAS detector, Phys. Rev. D 86 (2012), http://dx.doi.org/10.1103/PhysRevD.86.092002, 092002, arXiv:1208.4688.

[17] ATLAS Collaboration, Search for direct top squark pair production in final states with one isolated lepton, jets, and missing transverse momentum in $\sqrt{s} = 7$ TeV pp collisions using 4.7 fb^{-1} of ATLAS data, Phys. Rev. Lett. 109 (2012), http://dx.doi.org/10.1103/PhysRevLett.109.211803, 211803, arXiv:1208.2590.

[18] G.R. Farrar, P. Fayet, Phenomenology of the production, decay, and detection of new hadronic states associated with supersymmetry, Phys. Lett. B 76 (1978) 575, http://dx.doi.org/10.1016/0370-2693(78)90858-4.

[19] N. Arkani-Hamed, P. Schuster, N. Toro, J. Thaler, L.-T. Wang, B. Knuteson, S. Mrenna, MARMOSET: The path from LHC data to the new standard model via on-shell effective theories, arXiv:hep-ph/0703088, 2007.

[20] J. Alwall, P.C. Schuster, N. Toro, Simplified models for a first characterization of new physics at the LHC, Phys. Rev. D 79 (2009), http://dx.doi.org/10.1103/PhysRevD.79.075020, 075020, arXiv:0810.3921.

[21] D. Alves, et al., Simplified models for LHC new physics searches, J. Phys. G 39 (2012), http://dx.doi.org/10.1088/0954-3899/39/10/105005, 105005, arXiv:1105.2838.

[22] CMS Collaboration, The CMS experiment at the CERN LHC, J. Instrum. 03 (2008), http://dx.doi.org/10.1088/1748-0221/3/08/S08004, S08004.

[23] J. Alwall, M. Herquet, F. Maltoni, O. Mattelaer, T. Stelzer, MadGraph 5: going beyond, J. High Energy Phys. 06 (2011), http://dx.doi.org/10.1007/JHEP06(2011)128, 128, arXiv:1106.0522.

[24] J. Pumplin, D.R. Stump, J. Huston, H.-L. Lai, P. Nadolsky, W.-K. Tung, New generation of parton distributions with uncertainties from global QCD analysis, J. High Energy Phys. 07 (2002), http://dx.doi.org/10.1088/1126-6708/2002/07/012, 012, arXiv:hep-ph/0201195.

[25] S. Frixione, P. Nason, C. Oleari, Matching NLO QCD computations with parton shower simulations: the POWHEG method, J. High Energy Phys. 11 (2007), http://dx.doi.org/10.1088/1126-6708/2007/11/070, 070, arXiv:0709.2092.

[26] T. Sjöstrand, S. Mrenna, P.Z. Skands, PYTHIA 6.4 physics and manual, J. High Energy Phys. 05 (2006), http://dx.doi.org/10.1088/1126-6708/2006/05/026, 026, arXiv:hep-ph/0603175.

[27] CMS Collaboration, Measurement of the underlying event activity at the LHC with $\sqrt{s} = 7$ TeV and comparison with $\sqrt{s} = 0.9$ TeV, J. High Energy Phys. 09 (2011), http://dx.doi.org/10.1007/JHEP09(2011)109, 109, arXiv:1107.0330.

[28] Z. Wąs, TAUOLA the library for tau lepton decay, and KKMC/KORALB/KORALZ/… report, Nucl. Phys. B, Proc. Suppl. 98 (2001) 96, http://dx.doi.org/10.1016/S0920-5632(01)01200-2, arXiv:hep-ph/0011305.

[29] S. Agostinelli, et al., GEANT4 Collaboration, GEANT4—a simulation toolkit, Nucl. Instrum. Methods Phys. Res., Sect. A, Accel. Spectrom. Detect. Assoc. Equip. 506 (2003) 250, http://dx.doi.org/10.1016/S0168-9002(03)01368-8.

[30] CMS Collaboration, The fast simulation of the CMS detector at LHC, J. Phys. Conf. Ser. 331 (2011), http://dx.doi.org/10.1088/1742-6596/331/3/032049, 032049.

[31] CMS Collaboration, Electron reconstruction and identification at $\sqrt{s} = 7$ TeV, CMS Physics Analysis Summary CMS-PAS-EGM-10–004, 2010, http://cdsweb.cern.ch/record/1299116.

[32] CMS Collaboration, Performance of CMS muon reconstruction in pp collision events at $\sqrt{s} = 7$ TeV, J. Instrum. 7 (2012), http://dx.doi.org/10.1088/1748-0221/7/10/P10002, P10002, arXiv:1206.4071.

[33] CMS Collaboration, Measurement of the inclusive W and Z production cross sections in pp collisions at $\sqrt{s} = 7$ TeV, J. High Energy Phys. 10 (2011), http://dx.doi.org/10.1007/JHEP10(2011)132, 132, arXiv:1107.4789.

[34] CMS Collaboration, Commissioning of the particle-flow reconstruction in minimum-bias and jet events from pp collisions at 7 TeV, CMS Physics Analysis Summary CMS-PAS-PFT-10–002, 2010, http://cdsweb.cern.ch/record/1279341.

[35] M. Cacciari, G.P. Salam, G. Soyez, The anti-k_t jet clustering algorithm, J. High Energy Phys. 04 (2008), http://dx.doi.org/10.1088/1126-6708/2008/04/063, 063, arXiv:0802.1189.

[36] CMS Collaboration, Determination of jet energy calibration and transverse momentum resolution in CMS, J. Instrum. 6 (2011), http://dx.doi.org/10.1088/1748-0221/6/11/P11002, P11002, arXiv:1107.4277.

[37] CMS Collaboration, Identification of b-quark jets with the CMS experiment, J. Instrum. 8 (2013), http://dx.doi.org/10.1088/1748-0221/8/04/P04013, P04013, arXiv:1211.4462.

[38] CMS Collaboration, Performance of b tagging at $\sqrt{s} = 8$ TeV in multijet, $t\bar{t}$ and boosted topology events, CMS Physics Analysis Summary CMS-PAS-BTV-13–001, 2013, http://cds.cern.ch/record/1581306.

[39] V. Pavlunin, Modeling missing transverse energy in $V + $ jets at CERN LHC, Phys. Rev. D 81 (2010), http://dx.doi.org/10.1103/PhysRevD.81.035005, 035005, arXiv:0906.5016.

[40] A. Czarnecki, J.G. Körner, J.H. Piclum, Helicity fractions of W bosons from top quark decays at next-to-next-to-leading order in QCD, Phys. Rev. D 81 (2010), http://dx.doi.org/10.1103/PhysRevD.81.111503, 111503(R), arXiv:1005.2625.

[41] J. Pickands, Statistical inference using extreme order statistics, Ann. Stat. 3 (1975) 119, http://dx.doi.org/10.1214/aos/1176343003.

[42] CMS Collaboration, Measurement of the $Z/\gamma^* + $ b-jet cross section in pp collisions at $\sqrt{s} = 7$ TeV, J. High Energy Phys. 06 (2012), http://dx.doi.org/10.1007/JHEP06(2012)126, 126, arXiv:1204.1643.

[43] ATLAS Collaboration, Measurement of the cross-section for W boson production in association with b-jets in pp collisions at $\sqrt{s} = 7$ TeV with the ATLAS detector, J. High Energy Phys. 06 (2013), http://dx.doi.org/10.1007/JHEP06(2013)084, 084, arXiv:1302.2929.

[44] CMS Collaboration, Measurement of the t-channel single top quark production cross section in pp collisions at $\sqrt{s} = 7$ TeV, Phys. Rev. Lett. 107 (2011), http://dx.doi.org/10.1103/PhysRevLett.107.091802, 091802, arXiv:1106.3052.

[45] CMS Collaboration, Measurement of the polarization of W bosons with large transverse momenta in W + jets events at the LHC, Phys. Rev. Lett. 107 (2011), http://dx.doi.org/10.1103/PhysRevLett.107.021802, 021802, arXiv:1104.3829.

[46] M. Botje, J. Butterworth, A. Cooper-Sarkar, A. de Roeck, J. Feltesse, S. Forte, A. Glazov, J. Huston, R. McNulty, T. Sjöstrand, R. Thorne, The PDF4LHC working group interim recommendations, arXiv:1101.0538, 2011.

[47] CMS Collaboration, CMS luminosity based on pixel cluster counting – Summer 2013 update, CMS Physics Analysis Summary CMS-PAS-LUM-13–001, 2013, http://cds.cern.ch/record/1598864.

[48] T. Junk, Confidence level computation for combining searches with small statistics, Nucl. Instrum. Methods Phys. Res., Sect. A, Accel. Spectrom. Detect. Assoc. Equip. 434 (1999) 435, http://dx.doi.org/10.1016/S0168-9002(99)00498-2, arXiv:hep-ex/9902006.

[49] A.L. Read, Presentation of search results: the CLS technique, J. Phys. G 28 (2002) 2693, http://dx.doi.org/10.1088/0954-3899/28/10/313.

[50] ATLAS Collaboration, CMS Collaboration, LHC Higgs Combination Group, Procedure for the LHC Higgs boson search combination in Summer 2011, Technical Report ATL-PHYS-PUB/2011-11, CMS NOTE 2011/005, 2011, http://cdsweb.cern.ch/record/1379837.

[51] W. Beenakker, R. Höpker, M. Spira, P.M. Zerwas, Squark and gluino production at hadron colliders, Nucl. Phys. B 492 (1997) 51, http://dx.doi.org/10.1016/S0550-3213(97)80027-2, arXiv:hep-ph/9610490.

[52] A. Kulesza, L. Motyka, Threshold resummation for squark–antisquark and gluino-pair production at the LHC, Phys. Rev. Lett. 102 (2009), http://dx.doi.org/10.1103/PhysRevLett.102.111802, 111802, arXiv:0807.2405.

[53] A. Kulesza, L. Motyka, Soft gluon resummation for the production of gluino–gluino and squark–antisquark pairs at the LHC, Phys. Rev. D 80 (2009), http://dx.doi.org/10.1103/PhysRevD.80.095004, 095004, arXiv:0905.4749.

[54] W. Beenakker, S. Brensing, M. Krämer, A. Kulesza, E. Laenen, I. Niessen, Soft-gluon resummation for squark and gluino hadroproduction, J. High Energy Phys. 09 (2009), http://dx.doi.org/10.1088/1126-6708/2009/12/041, 041, arXiv:0909.4418.

[55] W. Beenakker, S. Brensing, M. Krämer, A. Kulesza, E. Laenen, L. Motyka, I. Niessen, Squark and gluino hadroproduction, Int. J. Mod. Phys. A 26 (2011) 2637, http://dx.doi.org/10.1142/S0217751X11053560, arXiv:1105.1110.

[56] M. Krämer, A. Kulesza, R. van der Leeuw, M. Mangano, S. Padhi, T. Plehn, X. Portell, Supersymmetry production cross sections in pp collisions at $\sqrt{s} =$ 7 TeV, arXiv:1206.2892, 2012.

CMS Collaboration

S. Chatrchyan, V. Khachatryan, A.M. Sirunyan, A. Tumasyan

Yerevan Physics Institute, Yerevan, Armenia

W. Adam, T. Bergauer, M. Dragicevic, J. Erö, C. Fabjan [1], M. Friedl, R. Frühwirth [1], V.M. Ghete, N. Hörmann, J. Hrubec, M. Jeitler [1], W. Kiesenhofer, V. Knünz, M. Krammer [1], I. Krätschmer, D. Liko, I. Mikulec, D. Rabady [2], B. Rahbaran, H. Rohringer, R. Schöfbeck, J. Strauss, A. Taurok, W. Treberer-Treberspurg, W. Waltenberger, C.-E. Wulz [1]

Institut für Hochenergiephysik der OeAW, Wien, Austria

V. Mossolov, N. Shumeiko, J. Suarez Gonzalez

National Centre for Particle and High Energy Physics, Minsk, Belarus

S. Alderweireldt, M. Bansal, S. Bansal, T. Cornelis, E.A. De Wolf, X. Janssen, A. Knutsson, S. Luyckx, L. Mucibello, S. Ochesanu, B. Roland, R. Rougny, Z. Staykova, H. Van Haevermaet, P. Van Mechelen, N. Van Remortel, A. Van Spilbeeck

Universiteit Antwerpen, Antwerpen, Belgium

F. Blekman, S. Blyweert, J. D'Hondt, N. Heracleous, A. Kalogeropoulos, J. Keaveney, S. Lowette, M. Maes, A. Olbrechts, D. Strom, S. Tavernier, W. Van Doninck, P. Van Mulders, G.P. Van Onsem, I. Villella

Vrije Universiteit Brussel, Brussel, Belgium

C. Caillol, B. Clerbaux, G. De Lentdecker, L. Favart, A.P.R. Gay, T. Hreus, A. Léonard, P.E. Marage, A. Mohammadi, L. Perniè, T. Reis, T. Seva, L. Thomas, C. Vander Velde, P. Vanlaer, J. Wang

Université Libre de Bruxelles, Bruxelles, Belgium

V. Adler, K. Beernaert, L. Benucci, A. Cimmino, S. Costantini, S. Dildick, G. Garcia, B. Klein, J. Lellouch, A. Marinov, J. Mccartin, A.A. Ocampo Rios, D. Ryckbosch, M. Sigamani, N. Strobbe, F. Thyssen, M. Tytgat, S. Walsh, E. Yazgan, N. Zaganidis

Ghent University, Ghent, Belgium

S. Basegmez, C. Beluffi [3], G. Bruno, R. Castello, A. Caudron, L. Ceard, G.G. Da Silveira, C. Delaere, T. du Pree, D. Favart, L. Forthomme, A. Giammanco [4], J. Hollar, P. Jez, V. Lemaitre, J. Liao, O. Militaru, C. Nuttens, D. Pagano, A. Pin, K. Piotrzkowski, A. Popov [5], M. Selvaggi, M. Vidal Marono, J.M. Vizan Garcia

Université Catholique de Louvain, Louvain-la-Neuve, Belgium

N. Beliy, T. Caebergs, E. Daubie, G.H. Hammad

Université de Mons, Mons, Belgium

G.A. Alves, M. Correa Martins Junior, T. Martins, M.E. Pol, M.H.G. Souza

Centro Brasileiro de Pesquisas Fisicas, Rio de Janeiro, Brazil

W.L. Aldá Júnior, W. Carvalho, J. Chinellato [6], A. Custódio, E.M. Da Costa, D. De Jesus Damiao, C. De Oliveira Martins, S. Fonseca De Souza, H. Malbouisson, M. Malek, D. Matos Figueiredo, L. Mundim, H. Nogima, W.L. Prado Da Silva, J. Santaolalla, A. Santoro, A. Sznajder, E.J. Tonelli Manganote [6], A. Vilela Pereira

Universidade do Estado do Rio de Janeiro, Rio de Janeiro, Brazil

C.A. Bernardes [b], F.A. Dias [a,7], T.R. Fernandez Perez Tomei [a], E.M. Gregores [b], C. Lagana [a], P.G. Mercadante [b], S.F. Novaes [a], Sandra S. Padula [a]

[a] *Universidade Estadual Paulista, São Paulo, Brazil*
[b] *Universidade Federal do ABC, São Paulo, Brazil*

V. Genchev [2], P. Iaydjiev [2], S. Piperov, M. Rodozov, G. Sultanov, M. Vutova

Institute for Nuclear Research and Nuclear Energy, Sofia, Bulgaria

A. Dimitrov, I. Glushkov, R. Hadjiiska, V. Kozhuharov, L. Litov, B. Pavlov, P. Petkov

University of Sofia, Sofia, Bulgaria

J.G. Bian, G.M. Chen, H.S. Chen, M. Chen, C.H. Jiang, D. Liang, S. Liang, X. Meng, R. Plestina [8], J. Tao, X. Wang, Z. Wang

Institute of High Energy Physics, Beijing, China

C. Asawatangtrakuldee, Y. Ban, Y. Guo, Q. Li, W. Li, S. Liu, Y. Mao, S.J. Qian, D. Wang, L. Zhang, W. Zou

State Key Laboratory of Nuclear Physics and Technology, Peking University, Beijing, China

C. Avila, C.A. Carrillo Montoya, L.F. Chaparro Sierra, C. Florez, J.P. Gomez, B. Gomez Moreno, J.C. Sanabria

Universidad de Los Andes, Bogota, Colombia

N. Godinovic, D. Lelas, D. Polic, I. Puljak

Technical University of Split, Split, Croatia

Z. Antunovic, M. Kovac

University of Split, Split, Croatia

V. Brigljevic, K. Kadija, J. Luetic, D. Mekterovic, S. Morovic, L. Tikvica

Institute Rudjer Boskovic, Zagreb, Croatia

A. Attikis, G. Mavromanolakis, J. Mousa, C. Nicolaou, F. Ptochos, P.A. Razis

University of Cyprus, Nicosia, Cyprus

M. Finger, M. Finger Jr.

Charles University, Prague, Czech Republic

A.A. Abdelalim [9], Y. Assran [10], S. Elgammal [9], A. Ellithi Kamel [11], M.A. Mahmoud [12], A. Radi [13,14]

Academy of Scientific Research and Technology of the Arab Republic of Egypt, Egyptian Network of High Energy Physics, Cairo, Egypt

M. Kadastik, M. Müntel, M. Murumaa, M. Raidal, L. Rebane, A. Tiko

National Institute of Chemical Physics and Biophysics, Tallinn, Estonia

P. Eerola, G. Fedi, M. Voutilainen

Department of Physics, University of Helsinki, Helsinki, Finland

J. Härkönen, V. Karimäki, R. Kinnunen, M.J. Kortelainen, T. Lampén, K. Lassila-Perini, S. Lehti, T. Lindén, P. Luukka, T. Mäenpää, T. Peltola, E. Tuominen, J. Tuominiemi, E. Tuovinen, L. Wendland

Helsinki Institute of Physics, Helsinki, Finland

T. Tuuva

Lappeenranta University of Technology, Lappeenranta, Finland

M. Besancon, F. Couderc, M. Dejardin, D. Denegri, B. Fabbro, J.L. Faure, F. Ferri, S. Ganjour, A. Givernaud, P. Gras, G. Hamel de Monchenault, P. Jarry, E. Locci, J. Malcles, A. Nayak, J. Rander, A. Rosowsky, M. Titov

DSM/IRFU, CEA/Saclay, Gif-sur-Yvette, France

S. Baffioni, F. Beaudette, L. Benhabib, M. Bluj [15], P. Busson, C. Charlot, N. Daci, T. Dahms, M. Dalchenko, L. Dobrzynski, A. Florent, R. Granier de Cassagnac, M. Haguenauer, P. Miné, C. Mironov, I.N. Naranjo, M. Nguyen, C. Ochando, P. Paganini, D. Sabes, R. Salerno, Y. Sirois, C. Veelken, A. Zabi

Laboratoire Leprince-Ringuet, Ecole Polytechnique, IN2P3–CNRS, Palaiseau, France

J.-L. Agram [16], J. Andrea, D. Bloch, J.-M. Brom, E.C. Chabert, C. Collard, E. Conte [16], F. Drouhin [16], J.-C. Fontaine [16], D. Gelé, U. Goerlach, C. Goetzmann, P. Juillot, A.-C. Le Bihan, P. Van Hove

Institut Pluridisciplinaire Hubert Curien, Université de Strasbourg, Université de Haute Alsace Mulhouse, CNRS/IN2P3, Strasbourg, France

S. Gadrat

Centre de Calcul de l'Institut National de Physique Nucléaire et de Physique des Particules, CNRS/IN2P3, Villeurbanne, France

S. Beauceron, N. Beaupere, G. Boudoul, S. Brochet, J. Chasserat, R. Chierici, D. Contardo, P. Depasse, H. El Mamouni, J. Fan, J. Fay, S. Gascon, M. Gouzevitch, B. Ille, T. Kurca, M. Lethuillier, L. Mirabito, S. Perries, J.D. Ruiz Alvarez [17], L. Sgandurra, V. Sordini, M. Vander Donckt, P. Verdier, S. Viret, H. Xiao

Université de Lyon, Université Claude Bernard Lyon 1, CNRS–IN2P3, Institut de Physique Nucléaire de Lyon, Villeurbanne, France

Z. Tsamalaidze [18]

Institute of High Energy Physics and Informatization, Tbilisi State University, Tbilisi, Georgia

C. Autermann, S. Beranek, M. Bontenackels, B. Calpas, M. Edelhoff, L. Feld, O. Hindrichs, K. Klein, A. Ostapchuk, A. Perieanu, F. Raupach, J. Sammet, S. Schael, D. Sprenger, H. Weber, B. Wittmer, V. Zhukov [5]

RWTH Aachen University, I. Physikalisches Institut, Aachen, Germany

M. Ata, J. Caudron, E. Dietz-Laursonn, D. Duchardt, M. Erdmann, R. Fischer, A. Güth, T. Hebbeker, C. Heidemann, K. Hoepfner, D. Klingebiel, S. Knutzen, P. Kreuzer, M. Merschmeyer, A. Meyer, M. Olschewski, K. Padeken, P. Papacz, H. Pieta, H. Reithler, S.A. Schmitz, L. Sonnenschein, D. Teyssier, S. Thüer, M. Weber

RWTH Aachen University, III. Physikalisches Institut A, Aachen, Germany

V. Cherepanov, Y. Erdogan, G. Flügge, H. Geenen, M. Geisler, W. Haj Ahmad, F. Hoehle, B. Kargoll, T. Kress, Y. Kuessel, J. Lingemann [2], A. Nowack, I.M. Nugent, L. Perchalla, O. Pooth, A. Stahl

RWTH Aachen University, III. Physikalisches Institut B, Aachen, Germany

I. Asin, N. Bartosik, J. Behr, W. Behrenhoff, U. Behrens, A.J. Bell, M. Bergholz [19], A. Bethani, K. Borras, A. Burgmeier, A. Cakir, L. Calligaris, A. Campbell, S. Choudhury, F. Costanza, C. Diez Pardos, S. Dooling, T. Dorland, G. Eckerlin, D. Eckstein, G. Flucke, A. Geiser, A. Grebenyuk, P. Gunnellini, S. Habib, J. Hauk, G. Hellwig, M. Hempel, D. Horton, H. Jung, M. Kasemann, P. Katsas, C. Kleinwort, H. Kluge, M. Krämer, D. Krücker, W. Lange, J. Leonard, K. Lipka, W. Lohmann [19], B. Lutz, R. Mankel, I. Marfin, I.-A. Melzer-Pellmann, A.B. Meyer, J. Mnich, A. Mussgiller, S. Naumann-Emme, O. Novgorodova, F. Nowak, J. Olzem, H. Perrey, A. Petrukhin, D. Pitzl, R. Placakyte, A. Raspereza, P.M. Ribeiro Cipriano, C. Riedl, E. Ron, M.Ö. Sahin, J. Salfeld-Nebgen, R. Schmidt [19], T. Schoerner-Sadenius, M. Schröder, N. Sen, M. Stein, R. Walsh, C. Wissing

Deutsches Elektronen-Synchrotron, Hamburg, Germany

M. Aldaya Martin, V. Blobel, H. Enderle, J. Erfle, E. Garutti, M. Görner, M. Gosselink, J. Haller, K. Heine, R.S. Höing, G. Kaussen, H. Kirschenmann, R. Klanner, R. Kogler, J. Lange, I. Marchesini, J. Ott, T. Peiffer, N. Pietsch, D. Rathjens, C. Sander, H. Schettler, P. Schleper, E. Schlieckau, A. Schmidt, T. Schum, M. Seidel, J. Sibille [20], V. Sola, H. Stadie, G. Steinbrück, D. Troendle, E. Usai, L. Vanelderen

University of Hamburg, Hamburg, Germany

C. Barth, C. Baus, J. Berger, C. Böser, E. Butz, T. Chwalek, W. De Boer, A. Descroix, A. Dierlamm, M. Feindt, M. Guthoff [2], F. Hartmann [2], T. Hauth [2], H. Held, K.H. Hoffmann, U. Husemann, I. Katkov [5], J.R. Komaragiri, A. Kornmayer [2], E. Kuznetsova, P. Lobelle Pardo, D. Martschei, M.U. Mozer, Th. Müller, M. Niegel, A. Nürnberg, O. Oberst, G. Quast, K. Rabbertz, F. Ratnikov, S. Röcker, F.-P. Schilling, G. Schott, H.J. Simonis, F.M. Stober, R. Ulrich, J. Wagner-Kuhr, S. Wayand, T. Weiler, M. Zeise

Institut für Experimentelle Kernphysik, Karlsruhe, Germany

G. Anagnostou, G. Daskalakis, T. Geralis, S. Kesisoglou, A. Kyriakis, D. Loukas, A. Markou, C. Markou, E. Ntomari, I. Topsis-giotis

Institute of Nuclear and Particle Physics (INPP), NCSR Demokritos, Aghia Paraskevi, Greece

L. Gouskos, A. Panagiotou, N. Saoulidou, E. Stiliaris

University of Athens, Athens, Greece

X. Aslanoglou, I. Evangelou, G. Flouris, C. Foudas, P. Kokkas, N. Manthos, I. Papadopoulos, E. Paradas

University of Ioánnina, Ioánnina, Greece

G. Bencze, C. Hajdu, P. Hidas, D. Horvath [21], F. Sikler, V. Veszpremi, G. Vesztergombi [22], A.J. Zsigmond

KFKI Research Institute for Particle and Nuclear Physics, Budapest, Hungary

N. Beni, S. Czellar, J. Molnar, J. Palinkas, Z. Szillasi

Institute of Nuclear Research ATOMKI, Debrecen, Hungary

J. Karancsi, P. Raics, Z.L. Trocsanyi, B. Ujvari

University of Debrecen, Debrecen, Hungary

S.K. Swain [23]

National Institute of Science Education and Research, Bhubaneswar, India

S.B. Beri, V. Bhatnagar, N. Dhingra, R. Gupta, M. Kaur, M.Z. Mehta, M. Mittal, N. Nishu, A. Sharma, J.B. Singh

Panjab University, Chandigarh, India

Ashok Kumar, Arun Kumar, S. Ahuja, A. Bhardwaj, B.C. Choudhary, A. Kumar, S. Malhotra, M. Naimuddin, K. Ranjan, P. Saxena, V. Sharma, R.K. Shivpuri

University of Delhi, Delhi, India

S. Banerjee, S. Bhattacharya, K. Chatterjee, S. Dutta, B. Gomber, Sa. Jain, Sh. Jain, R. Khurana, A. Modak, S. Mukherjee, D. Roy, S. Sarkar, M. Sharan, A.P. Singh

Saha Institute of Nuclear Physics, Kolkata, India

A. Abdulsalam, D. Dutta, S. Kailas, V. Kumar, A.K. Mohanty [2], L.M. Pant, P. Shukla, A. Topkar

Bhabha Atomic Research Centre, Mumbai, India

T. Aziz, R.M. Chatterjee, S. Ganguly, S. Ghosh, M. Guchait [24], A. Gurtu [25], G. Kole, S. Kumar, M. Maity [26], G. Majumder, K. Mazumdar, G.B. Mohanty, B. Parida, K. Sudhakar, N. Wickramage [27]

Tata Institute of Fundamental Research – EHEP, Mumbai, India

S. Banerjee, S. Dugad

Tata Institute of Fundamental Research – HECR, Mumbai, India

H. Arfaei, H. Bakhshiansohi, S.M. Etesami [28], A. Fahim [29], A. Jafari, M. Khakzad, M. Mohammadi Najafabadi, S. Paktinat Mehdiabadi, B. Safarzadeh [30], M. Zeinali

Institute for Research in Fundamental Sciences (IPM), Tehran, Iran

M. Grunewald

University College Dublin, Dublin, Ireland

M. Abbrescia [a,b], L. Barbone [a,b], C. Calabria [a,b], S.S. Chhibra [a,b], A. Colaleo [a], D. Creanza [a,c], N. De Filippis [a,c], M. De Palma [a,b], L. Fiore [a], G. Iaselli [a,c], G. Maggi [a,c], M. Maggi [a], B. Marangelli [a,b], S. My [a,c], S. Nuzzo [a,b], N. Pacifico [a], A. Pompili [a,b], G. Pugliese [a,c], R. Radogna [a,b], G. Selvaggi [a,b], L. Silvestris [a], G. Singh [a,b], R. Venditti [a,b], P. Verwilligen [a], G. Zito [a]

[a] *INFN Sezione di Bari, Bari, Italy*
[b] *Università di Bari, Bari, Italy*
[c] *Politecnico di Bari, Bari, Italy*

G. Abbiendi [a], A.C. Benvenuti [a], D. Bonacorsi [a,b], S. Braibant-Giacomelli [a,b], L. Brigliadori [a,b], R. Campanini [a,b], P. Capiluppi [a,b], A. Castro [a,b], F.R. Cavallo [a], G. Codispoti [a,b], M. Cuffiani [a,b], G.M. Dallavalle [a], F. Fabbri [a], A. Fanfani [a,b], D. Fasanella [a,b], P. Giacomelli [a], C. Grandi [a], L. Guiducci [a,b], S. Marcellini [a], G. Masetti [a], M. Meneghelli [a,b], A. Montanari [a], F.L. Navarria [a,b], F. Odorici [a], A. Perrotta [a], F. Primavera [a,b], A.M. Rossi [a,b], T. Rovelli [a,b], G.P. Siroli [a,b], N. Tosi [a,b], R. Travaglini [a,b]

[a] *INFN Sezione di Bologna, Bologna, Italy*
[b] *Università di Bologna, Bologna, Italy*

S. Albergo [a,b], G. Cappello [a], M. Chiorboli [a,b], S. Costa [a,b], F. Giordano [a,2], R. Potenza [a,b], A. Tricomi [a,b], C. Tuve [a,b]

[a] *INFN Sezione di Catania, Catania, Italy*
[b] *Università di Catania, Catania, Italy*

G. Barbagli [a], V. Ciulli [a,b], C. Civinini [a], R. D'Alessandro [a,b], E. Focardi [a,b], E. Gallo [a], S. Gonzi [a,b], V. Gori [a,b], P. Lenzi [a,b], M. Meschini [a], S. Paoletti [a], G. Sguazzoni [a], A. Tropiano [a,b]

[a] *INFN Sezione di Firenze, Firenze, Italy*
[b] *Università di Firenze, Firenze, Italy*

L. Benussi, S. Bianco, F. Fabbri, D. Piccolo

INFN Laboratori Nazionali di Frascati, Frascati, Italy

P. Fabbricatore [a], R. Ferretti [a,b], F. Ferro [a], M. Lo Vetere [a,b], R. Musenich [a], E. Robutti [a], S. Tosi [a,b]

[a] *INFN Sezione di Genova, Genova, Italy*
[b] *Università di Genova, Genova, Italy*

A. Benaglia [a], M.E. Dinardo [a,b], S. Fiorendi [a,b,2], S. Gennai [a], A. Ghezzi [a,b], P. Govoni [a,b], M.T. Lucchini [a,b,2], S. Malvezzi [a], R.A. Manzoni [a,b,2], A. Martelli [a,b,2], D. Menasce [a], L. Moroni [a], M. Paganoni [a,b], D. Pedrini [a], S. Ragazzi [a,b], N. Redaelli [a], T. Tabarelli de Fatis [a,b]

[a] *INFN Sezione di Milano-Bicocca, Milano, Italy*
[b] *Università di Milano-Bicocca, Milano, Italy*

S. Buontempo [a], N. Cavallo [a,c], F. Fabozzi [a,c], A.O.M. Iorio [a,b], L. Lista [a], S. Meola [a,d,2], M. Merola [a], P. Paolucci [a,2]

[a] *INFN Sezione di Napoli, Napoli, Italy*
[b] *Università di Napoli 'Federico II', Napoli, Italy*
[c] *Università della Basilicata (Potenza), Napoli, Italy*
[d] *Università G. Marconi (Roma), Napoli, Italy*

P. Azzi [a], N. Bacchetta [a], D. Bisello [a,b], A. Branca [a,b], R. Carlin [a,b], P. Checchia [a], T. Dorigo [a], U. Dosselli [a], M. Galanti [a,b,2], F. Gasparini [a,b], U. Gasparini [a,b], P. Giubilato [a,b], F. Gonella [a], A. Gozzelino [a], K. Kanishchev [a,c], S. Lacaprara [a], I. Lazzizzera [a,c], M. Margoni [a,b], A.T. Meneguzzo [a,b], F. Montecassiano [a], J. Pazzini [a,b], N. Pozzobon [a,b], P. Ronchese [a,b], F. Simonetto [a,b], E. Torassa [a], M. Tosi [a,b], S. Ventura [a], P. Zotto [a,b], A. Zucchetta [a,b], G. Zumerle [a,b]

[a] *INFN Sezione di Padova, Padova, Italy*
[b] *Università di Padova, Padova, Italy*
[c] *Università di Trento (Trento), Padova, Italy*

M. Gabusi [a,b], S.P. Ratti [a,b], C. Riccardi [a,b], P. Vitulo [a,b]

[a] *INFN Sezione di Pavia, Pavia, Italy*
[b] *Università di Pavia, Pavia, Italy*

M. Biasini [a,b], G.M. Bilei [a], L. Fanò [a,b], P. Lariccia [a,b], G. Mantovani [a,b], M. Menichelli [a], A. Nappi [a,b,†], F. Romeo [a,b], A. Saha [a], A. Santocchia [a,b], A. Spiezia [a,b]

[a] *INFN Sezione di Perugia, Perugia, Italy*
[b] *Università di Perugia, Perugia, Italy*

K. Androsov [a,31], P. Azzurri [a], G. Bagliesi [a], J. Bernardini [a], T. Boccali [a], G. Broccolo [a,c], R. Castaldi [a], M.A. Ciocci [a,31], R. Dell'Orso [a], F. Fiori [a,c], L. Foà [a,c], A. Giassi [a], M.T. Grippo [a,31], A. Kraan [a], F. Ligabue [a,c], T. Lomtadze [a], L. Martini [a,b], A. Messineo [a,b], C.S. Moon [a,32], F. Palla [a], A. Rizzi [a,b], A. Savoy-Navarro [a,33], A.T. Serban [a], P. Spagnolo [a], P. Squillacioti [a,31], R. Tenchini [a], G. Tonelli [a,b], A. Venturi [a], P.G. Verdini [a], C. Vernieri [a,c]

[a] *INFN Sezione di Pisa, Pisa, Italy*
[b] *Università di Pisa, Pisa, Italy*
[c] *Scuola Normale Superiore di Pisa, Pisa, Italy*

L. Barone [a,b], F. Cavallari [a], D. Del Re [a,b], M. Diemoz [a], M. Grassi [a,b], C. Jorda [a], E. Longo [a,b], F. Margaroli [a,b], P. Meridiani [a], F. Micheli [a,b], S. Nourbakhsh [a,b], G. Organtini [a,b], R. Paramatti [a], S. Rahatlou [a,b], C. Rovelli [a], L. Soffi [a,b], P. Traczyk [a,b]

[a] *INFN Sezione di Roma, Roma, Italy*
[b] *Università di Roma, Roma, Italy*

N. Amapane [a,b], R. Arcidiacono [a,c], S. Argiro [a,b], M. Arneodo [a,c], R. Bellan [a,b], C. Biino [a], N. Cartiglia [a], S. Casasso [a,b], M. Costa [a,b], A. Degano [a,b], N. Demaria [a], C. Mariotti [a], S. Maselli [a], E. Migliore [a,b], V. Monaco [a,b], M. Musich [a], M.M. Obertino [a,c], G. Ortona [a,b], L. Pacher [a,b], N. Pastrone [a], M. Pelliccioni [a,2], A. Potenza [a,b], A. Romero [a,b], M. Ruspa [a,c], R. Sacchi [a,b], A. Solano [a,b], A. Staiano [a], U. Tamponi [a]

[a] *INFN Sezione di Torino, Torino, Italy*
[b] *Università di Torino, Torino, Italy*

[c] *Università del Piemonte Orientale (Novara), Torino, Italy*

S. Belforte [a], V. Candelise [a,b], M. Casarsa [a], F. Cossutti [a,2], G. Della Ricca [a,b], B. Gobbo [a], C. La Licata [a,b], M. Marone [a,b], D. Montanino [a,b], A. Penzo [a], A. Schizzi [a,b], T. Umer [a,b], A. Zanetti [a]

[a] *INFN Sezione di Trieste, Trieste, Italy*
[b] *Università di Trieste, Trieste, Italy*

S. Chang, T.Y. Kim, S.K. Nam

Kangwon National University, Chunchon, Republic of Korea

D.H. Kim, G.N. Kim, J.E. Kim, D.J. Kong, S. Lee, Y.D. Oh, H. Park, D.C. Son

Kyungpook National University, Daegu, Republic of Korea

J.Y. Kim, Zero J. Kim, S. Song

Chonnam National University, Institute for Universe and Elementary Particles, Kwangju, Republic of Korea

S. Choi, D. Gyun, B. Hong, M. Jo, H. Kim, T.J. Kim, Y. Kim, K.S. Lee, S.K. Park, Y. Roh

Korea University, Seoul, Republic of Korea

M. Choi, J.H. Kim, C. Park, I.C. Park, S. Park, G. Ryu

University of Seoul, Seoul, Republic of Korea

Y. Choi, Y.K. Choi, J. Goh, M.S. Kim, E. Kwon, B. Lee, J. Lee, S. Lee, H. Seo, I. Yu

Sungkyunkwan University, Suwon, Republic of Korea

I. Grigelionis, A. Juodagalvis

Vilnius University, Vilnius, Lithuania

H. Castilla-Valdez, E. De La Cruz-Burelo, I. Heredia-de La Cruz [34], R. Lopez-Fernandez, J. Martínez-Ortega, A. Sanchez-Hernandez, L.M. Villasenor-Cendejas

Centro de Investigacion y de Estudios Avanzados del IPN, Mexico City, Mexico

S. Carrillo Moreno, F. Vazquez Valencia

Universidad Iberoamericana, Mexico City, Mexico

H.A. Salazar Ibarguen

Benemerita Universidad Autonoma de Puebla, Puebla, Mexico

E. Casimiro Linares, A. Morelos Pineda

Universidad Autónoma de San Luis Potosí, San Luis Potosí, Mexico

D. Krofcheck

University of Auckland, Auckland, New Zealand

P.H. Butler, R. Doesburg, S. Reucroft, H. Silverwood

University of Canterbury, Christchurch, New Zealand

M. Ahmad, M.I. Asghar, J. Butt, H.R. Hoorani, S. Khalid, W.A. Khan, T. Khurshid, S. Qazi, M.A. Shah, M. Shoaib

National Centre for Physics, Quaid-I-Azam University, Islamabad, Pakistan

H. Bialkowska, B. Boimska, T. Frueboes, M. Górski, M. Kazana, K. Nawrocki, K. Romanowska-Rybinska, M. Szleper, G. Wrochna, P. Zalewski

National Centre for Nuclear Research, Swierk, Poland

G. Brona, K. Bunkowski, M. Cwiok, W. Dominik, K. Doroba, A. Kalinowski, M. Konecki, J. Krolikowski, M. Misiura, W. Wolszczak

Institute of Experimental Physics, Faculty of Physics, University of Warsaw, Warsaw, Poland

N. Almeida, P. Bargassa, C. Beirão Da Cruz E Silva, P. Faccioli, P.G. Ferreira Parracho, M. Gallinaro, F. Nguyen, J. Rodrigues Antunes, J. Seixas [2], J. Varela, P. Vischia

Laboratório de Instrumentação e Física Experimental de Partículas, Lisboa, Portugal

S. Afanasiev, P. Bunin, M. Gavrilenko, I. Golutvin, I. Gorbunov, A. Kamenev, V. Karjavin, V. Konoplyanikov, A. Lanev, A. Malakhov, V. Matveev, P. Moisenz, V. Palichik, V. Perelygin, S. Shmatov, N. Skatchkov, V. Smirnov, A. Zarubin

Joint Institute for Nuclear Research, Dubna, Russia

S. Evstyukhin, V. Golovtsov, Y. Ivanov, V. Kim, P. Levchenko, V. Murzin, V. Oreshkin, I. Smirnov, V. Sulimov, L. Uvarov, S. Vavilov, A. Vorobyev, An. Vorobyev

Petersburg Nuclear Physics Institute, Gatchina (St. Petersburg), Russia

Yu. Andreev, A. Dermenev, S. Gninenko, N. Golubev, M. Kirsanov, N. Krasnikov, A. Pashenkov, D. Tlisov, A. Toropin

Institute for Nuclear Research, Moscow, Russia

V. Epshteyn, V. Gavrilov, N. Lychkovskaya, V. Popov, G. Safronov, S. Semenov, A. Spiridonov, V. Stolin, E. Vlasov, A. Zhokin

Institute for Theoretical and Experimental Physics, Moscow, Russia

V. Andreev, M. Azarkin, I. Dremin, M. Kirakosyan, A. Leonidov, G. Mesyats, S.V. Rusakov, A. Vinogradov

P.N. Lebedev Physical Institute, Moscow, Russia

A. Belyaev, E. Boos, M. Dubinin [7], L. Dudko, A. Ershov, A. Gribushin, V. Klyukhin, O. Kodolova, I. Lokhtin, A. Markina, S. Obraztsov, S. Petrushanko, V. Savrin, A. Snigirev

Skobeltsyn Institute of Nuclear Physics, Lomonosov Moscow State University, Moscow, Russia

I. Azhgirey, I. Bayshev, S. Bitioukov, V. Kachanov, A. Kalinin, D. Konstantinov, V. Krychkine, V. Petrov, R. Ryutin, A. Sobol, L. Tourtchanovitch, S. Troshin, N. Tyurin, A. Uzunian, A. Volkov

State Research Center of Russian Federation, Institute for High Energy Physics, Protvino, Russia

P. Adzic [35], M. Djordjevic, M. Ekmedzic, J. Milosevic

University of Belgrade, Faculty of Physics and Vinca Institute of Nuclear Sciences, Belgrade, Serbia

M. Aguilar-Benitez, J. Alcaraz Maestre, C. Battilana, E. Calvo, M. Cerrada, M. Chamizo Llatas [2], N. Colino, B. De La Cruz, A. Delgado Peris, D. Domínguez Vázquez, C. Fernandez Bedoya, J.P. Fernández Ramos, A. Ferrando, J. Flix, M.C. Fouz, P. Garcia-Abia, O. Gonzalez Lopez, S. Goy Lopez, J.M. Hernandez, M.I. Josa, G. Merino, E. Navarro De Martino, J. Puerta Pelayo, A. Quintario Olmeda, I. Redondo, L. Romero, M.S. Soares, C. Willmott

Centro de Investigaciones Energéticas Medioambientales y Tecnológicas (CIEMAT), Madrid, Spain

C. Albajar, J.F. de Trocóniz

Universidad Autónoma de Madrid, Madrid, Spain

H. Brun, J. Cuevas, J. Fernandez Menendez, S. Folgueras, I. Gonzalez Caballero, L. Lloret Iglesias

Universidad de Oviedo, Oviedo, Spain

J.A. Brochero Cifuentes, I.J. Cabrillo, A. Calderon, S.H. Chuang, J. Duarte Campderros, M. Fernandez, G. Gomez, J. Gonzalez Sanchez, A. Graziano, A. Lopez Virto, J. Marco, R. Marco, C. Martinez Rivero, F. Matorras, F.J. Munoz Sanchez, J. Piedra Gomez, T. Rodrigo, A.Y. Rodríguez-Marrero, A. Ruiz-Jimeno, L. Scodellaro, I. Vila, R. Vilar Cortabitarte

Instituto de Física de Cantabria (IFCA), CSIC–Universidad de Cantabria, Santander, Spain

D. Abbaneo, E. Auffray, G. Auzinger, M. Bachtis, P. Baillon, A.H. Ball, D. Barney, J. Bendavid, J.F. Benitez, C. Bernet [8], G. Bianchi, P. Bloch, A. Bocci, A. Bonato, O. Bondu, C. Botta, H. Breuker, T. Camporesi, G. Cerminara, T. Christiansen, J.A. Coarasa Perez, S. Colafranceschi [36], M. D'Alfonso, D. d'Enterria, A. Dabrowski, A. David, F. De Guio, A. De Roeck, S. De Visscher, S. Di Guida, M. Dobson, N. Dupont-Sagorin, A. Elliott-Peisert, J. Eugster, G. Franzoni, W. Funk, M. Giffels, D. Gigi, K. Gill, D. Giordano, M. Girone, M. Giunta, F. Glege, R. Gomez-Reino Garrido, S. Gowdy, R. Guida, J. Hammer, M. Hansen, P. Harris, C. Hartl, A. Hinzmann, V. Innocente, P. Janot, E. Karavakis, K. Kousouris, K. Krajczar, P. Lecoq, Y.-J. Lee, C. Lourenço, N. Magini, L. Malgeri, M. Mannelli, L. Masetti, F. Meijers, S. Mersi, E. Meschi, M. Mulders, P. Musella, L. Orsini, E. Palencia Cortezon, E. Perez, L. Perrozzi, A. Petrilli, G. Petrucciani, A. Pfeiffer, M. Pierini, M. Pimiä, D. Piparo, M. Plagge, L. Quertenmont, A. Racz, W. Reece, G. Rolandi [37], M. Rovere, H. Sakulin, F. Santanastasio, C. Schäfer, C. Schwick, S. Sekmen, A. Sharma, P. Siegrist, P. Silva, M. Simon, P. Sphicas [38], D. Spiga, J. Steggemann, B. Stieger, M. Stoye, A. Tsirou, G.I. Veres [22], J.R. Vlimant, H.K. Wöhri, W.D. Zeuner

CERN, European Organization for Nuclear Research, Geneva, Switzerland

W. Bertl, K. Deiters, W. Erdmann, K. Gabathuler, R. Horisberger, Q. Ingram, H.C. Kaestli, S. König, D. Kotlinski, U. Langenegger, D. Renker, T. Rohe

Paul Scherrer Institut, Villigen, Switzerland

F. Bachmair, L. Bäni, L. Bianchini, P. Bortignon, M.A. Buchmann, B. Casal, N. Chanon, A. Deisher, G. Dissertori, M. Dittmar, M. Donegà, M. Dünser, P. Eller, K. Freudenreich, C. Grab, D. Hits, P. Lecomte, W. Lustermann, B. Mangano, A.C. Marini, P. Martinez Ruiz del Arbol, D. Meister, N. Mohr, F. Moortgat, C. Nägeli [39], P. Nef, F. Nessi-Tedaldi, F. Pandolfi, L. Pape, F. Pauss, M. Peruzzi, M. Quittnat, F.J. Ronga, M. Rossini, L. Sala, A. Starodumov [40], M. Takahashi, L. Tauscher [†], K. Theofilatos, D. Treille, R. Wallny, H.A. Weber

Institute for Particle Physics, ETH Zurich, Zurich, Switzerland

C. Amsler [41], V. Chiochia, A. De Cosa, C. Favaro, M. Ivova Rikova, B. Kilminster, B. Millan Mejias, J. Ngadiuba, P. Robmann, H. Snoek, S. Taroni, M. Verzetti, Y. Yang

Universität Zürich, Zurich, Switzerland

M. Cardaci, K.H. Chen, C. Ferro, C.M. Kuo, S.W. Li, W. Lin, Y.J. Lu, R. Volpe, S.S. Yu

National Central University, Chung-Li, Taiwan

P. Bartalini, P. Chang, Y.H. Chang, Y.W. Chang, Y. Chao, K.F. Chen, C. Dietz, U. Grundler, W.-S. Hou, Y. Hsiung, K.Y. Kao, Y.J. Lei, Y.F. Liu, R.-S. Lu, D. Majumder, E. Petrakou, X. Shi, J.G. Shiu, Y.M. Tzeng, M. Wang

National Taiwan University (NTU), Taipei, Taiwan

B. Asavapibhop, N. Suwonjandee

Chulalongkorn University, Bangkok, Thailand

A. Adiguzel, M.N. Bakirci [42], S. Cerci [43], C. Dozen, I. Dumanoglu, E. Eskut, S. Girgis, G. Gokbulut, E. Gurpinar, I. Hos, E.E. Kangal, A. Kayis Topaksu, G. Onengut [44], K. Ozdemir, S. Ozturk [42], A. Polatoz, K. Sogut [45], D. Sunar Cerci [43], B. Tali [43], H. Topakli [42], M. Vergili

Cukurova University, Adana, Turkey

I.V. Akin, T. Aliev, B. Bilin, S. Bilmis, M. Deniz, H. Gamsizkan, A.M. Guler, G. Karapinar [46], K. Ocalan, A. Ozpineci, M. Serin, R. Sever, U.E. Surat, M. Yalvac, M. Zeyrek

Middle East Technical University, Physics Department, Ankara, Turkey

E. Gülmez, B. Isildak [47], M. Kaya [48], O. Kaya [48], S. Ozkorucuklu [49], N. Sonmez [50]

Bogazici University, Istanbul, Turkey

H. Bahtiyar [51], E. Barlas, K. Cankocak, Y.O. Günaydin [52], F.I. Vardarlı, M. Yücel

Istanbul Technical University, Istanbul, Turkey

L. Levchuk, P. Sorokin

National Scientific Center, Kharkov Institute of Physics and Technology, Kharkov, Ukraine

J.J. Brooke, E. Clement, D. Cussans, H. Flacher, R. Frazier, J. Goldstein, M. Grimes, G.P. Heath, H.F. Heath, J. Jacob, L. Kreczko, C. Lucas, Z. Meng, S. Metson, D.M. Newbold [53], K. Nirunpong, S. Paramesvaran, A. Poll, S. Senkin, V.J. Smith, T. Williams

University of Bristol, Bristol, United Kingdom

K.W. Bell, A. Belyaev [54], C. Brew, R.M. Brown, D.J.A. Cockerill, J.A. Coughlan, K. Harder, S. Harper, J. Ilic, E. Olaiya, D. Petyt, C.H. Shepherd-Themistocleous, A. Thea, I.R. Tomalin, W.J. Womersley, S.D. Worm

Rutherford Appleton Laboratory, Didcot, United Kingdom

R. Bainbridge, O. Buchmuller, D. Burton, D. Colling, N. Cripps, M. Cutajar, P. Dauncey, G. Davies, M. Della Negra, W. Ferguson, J. Fulcher, D. Futyan, A. Gilbert, A. Guneratne Bryer, G. Hall, Z. Hatherell, J. Hays, G. Iles, M. Jarvis, G. Karapostoli, M. Kenzie, R. Lane, R. Lucas [53], L. Lyons, A.-M. Magnan, J. Marrouche, B. Mathias, R. Nandi, J. Nash, A. Nikitenko [40], J. Pela, M. Pesaresi, K. Petridis, M. Pioppi [55], D.M. Raymond, S. Rogerson, A. Rose, C. Seez, P. Sharp [†], A. Sparrow, A. Tapper, M. Vazquez Acosta, T. Virdee, S. Wakefield, N. Wardle

Imperial College, London, United Kingdom

J.E. Cole, P.R. Hobson, A. Khan, P. Kyberd, D. Leggat, D. Leslie, W. Martin, I.D. Reid, P. Symonds, L. Teodorescu, M. Turner

Brunel University, Uxbridge, United Kingdom

J. Dittmann, K. Hatakeyama, A. Kasmi, H. Liu, T. Scarborough

Baylor University, Waco, USA

O. Charaf, S.I. Cooper, C. Henderson, P. Rumerio

The University of Alabama, Tuscaloosa, USA

A. Avetisyan, T. Bose, C. Fantasia, A. Heister, P. Lawson, D. Lazic, J. Rohlf, D. Sperka, J. St. John, L. Sulak

Boston University, Boston, USA

J. Alimena, S. Bhattacharya, G. Christopher, D. Cutts, Z. Demiragli, A. Ferapontov, A. Garabedian, U. Heintz, S. Jabeen, G. Kukartsev, E. Laird, G. Landsberg, M. Luk, M. Narain, M. Segala, T. Sinthuprasith, T. Speer

Brown University, Providence, USA

R. Breedon, G. Breto, M. Calderon De La Barca Sanchez, S. Chauhan, M. Chertok, J. Conway, R. Conway, P.T. Cox, R. Erbacher, M. Gardner, W. Ko, A. Kopecky, R. Lander, T. Miceli, D. Pellett, J. Pilot, F. Ricci-Tam, B. Rutherford, M. Searle, S. Shalhout, J. Smith, M. Squires, M. Tripathi, S. Wilbur, R. Yohay

University of California, Davis, Davis, USA

V. Andreev, D. Cline, R. Cousins, S. Erhan, P. Everaerts, C. Farrell, M. Felcini, J. Hauser, M. Ignatenko, C. Jarvis, G. Rakness, P. Schlein [†], E. Takasugi, V. Valuev, M. Weber

University of California, Los Angeles, USA

J. Babb, R. Clare, J. Ellison, J.W. Gary, G. Hanson, J. Heilman, P. Jandir, F. Lacroix, H. Liu, O.R. Long, A. Luthra, M. Malberti, H. Nguyen, A. Shrinivas, J. Sturdy, S. Sumowidagdo, R. Wilken, S. Wimpenny

University of California, Riverside, Riverside, USA

W. Andrews, J.G. Branson, G.B. Cerati, S. Cittolin, R.T. D'Agnolo, D. Evans, A. Holzner, R. Kelley, D. Kovalskyi, M. Lebourgeois, J. Letts, I. Macneill, S. Padhi, C. Palmer, M. Pieri, M. Sani, V. Sharma, S. Simon, E. Sudano, M. Tadel, Y. Tu, A. Vartak, S. Wasserbaech [56], F. Würthwein, A. Yagil, J. Yoo

University of California, San Diego, La Jolla, USA

D. Barge, C. Campagnari, T. Danielson, K. Flowers, P. Geffert, C. George, F. Golf, J. Incandela, C. Justus, V. Krutelyov, R. Magaña Villalba, N. Mccoll, V. Pavlunin, J. Richman, R. Rossin, D. Stuart, W. To, C. West

University of California, Santa Barbara, Santa Barbara, USA

A. Apresyan, A. Bornheim, J. Bunn, Y. Chen, E. Di Marco, J. Duarte, D. Kcira, Y. Ma, A. Mott, H.B. Newman, C. Pena, C. Rogan, M. Spiropulu, V. Timciuc, R. Wilkinson, S. Xie, R.Y. Zhu

California Institute of Technology, Pasadena, USA

V. Azzolini, A. Calamba, R. Carroll, T. Ferguson, Y. Iiyama, D.W. Jang, M. Paulini, J. Russ, H. Vogel, I. Vorobiev

Carnegie Mellon University, Pittsburgh, USA

J.P. Cumalat, B.R. Drell, W.T. Ford, A. Gaz, E. Luiggi Lopez, U. Nauenberg, J.G. Smith, K. Stenson, K.A. Ulmer, S.R. Wagner

University of Colorado at Boulder, Boulder, USA

J. Alexander, A. Chatterjee, N. Eggert, L.K. Gibbons, W. Hopkins, A. Khukhunaishvili, B. Kreis, N. Mirman, G. Nicolas Kaufman, J.R. Patterson, A. Ryd, E. Salvati, W. Sun, W.D. Teo, J. Thom, J. Thompson, J. Tucker, Y. Weng, L. Winstrom, P. Wittich

Cornell University, Ithaca, USA

D. Winn

Fairfield University, Fairfield, USA

S. Abdullin, M. Albrow, J. Anderson, G. Apollinari, L.A.T. Bauerdick, A. Beretvas, J. Berryhill, P.C. Bhat, K. Burkett, J.N. Butler, V. Chetluru, H.W.K. Cheung, F. Chlebana, S. Cihangir, V.D. Elvira, I. Fisk, J. Freeman, Y. Gao, E. Gottschalk, L. Gray, D. Green, O. Gutsche, D. Hare, R.M. Harris, J. Hirschauer, B. Hooberman, S. Jindariani, M. Johnson, U. Joshi, K. Kaadze, B. Klima, S. Kwan, J. Linacre, D. Lincoln, R. Lipton, J. Lykken, K. Maeshima, J.M. Marraffino, V.I. Martinez Outschoorn, S. Maruyama, D. Mason, P. McBride, K. Mishra, S. Mrenna, Y. Musienko [57], C. Newman-Holmes, V. O'Dell, O. Prokofyev, N. Ratnikova, E. Sexton-Kennedy, S. Sharma, W.J. Spalding, L. Spiegel, L. Taylor, S. Tkaczyk, N.V. Tran, L. Uplegger, E.W. Vaandering, R. Vidal, J. Whitmore, W. Wu, F. Yang, J.C. Yun

Fermi National Accelerator Laboratory, Batavia, USA

D. Acosta, P. Avery, D. Bourilkov, T. Cheng, S. Das, M. De Gruttola, G.P. Di Giovanni, D. Dobur, A. Drozdetskiy, R.D. Field, M. Fisher, Y. Fu, I.K. Furic, J. Hugon, B. Kim, J. Konigsberg, A. Korytov, A. Kropivnitskaya, T. Kypreos, J.F. Low, K. Matchev, P. Milenovic [58], G. Mitselmakher, L. Muniz, A. Rinkevicius, N. Skhirtladze, M. Snowball, J. Yelton, M. Zakaria

University of Florida, Gainesville, USA

V. Gaultney, S. Hewamanage, S. Linn, P. Markowitz, G. Martinez, J.L. Rodriguez

Florida International University, Miami, USA

T. Adams, A. Askew, J. Bochenek, J. Chen, B. Diamond, J. Haas, S. Hagopian, V. Hagopian, K.F. Johnson, H. Prosper, V. Veeraraghavan, M. Weinberg

Florida State University, Tallahassee, USA

M.M. Baarmand, B. Dorney, M. Hohlmann, H. Kalakhety, F. Yumiceva

Florida Institute of Technology, Melbourne, USA

M.R. Adams, L. Apanasevich, V.E. Bazterra, R.R. Betts, I. Bucinskaite, J. Callner, R. Cavanaugh, O. Evdokimov, L. Gauthier, C.E. Gerber, D.J. Hofman, S. Khalatyan, P. Kurt, D.H. Moon, C. O'Brien, C. Silkworth, P. Turner, N. Varelas

University of Illinois at Chicago (UIC), Chicago, USA

U. Akgun, E.A. Albayrak [51], B. Bilki [59], W. Clarida, K. Dilsiz, F. Duru, J.-P. Merlo, H. Mermerkaya [60], A. Mestvirishvili, A. Moeller, J. Nachtman, H. Ogul, Y. Onel, F. Ozok [51], S. Sen, P. Tan, E. Tiras, J. Wetzel, T. Yetkin [61], K. Yi

The University of Iowa, Iowa City, USA

B.A. Barnett, B. Blumenfeld, S. Bolognesi, D. Fehling, A.V. Gritsan, P. Maksimovic, C. Martin, M. Swartz, A. Whitbeck

Johns Hopkins University, Baltimore, USA

P. Baringer, A. Bean, G. Benelli, R.P. Kenny III, M. Murray, D. Noonan, S. Sanders, J. Sekaric, R. Stringer, J.S. Wood

The University of Kansas, Lawrence, USA

A.F. Barfuss, I. Chakaberia, A. Ivanov, S. Khalil, M. Makouski, Y. Maravin, L.K. Saini, S. Shrestha, I. Svintradze

Kansas State University, Manhattan, USA

J. Gronberg, D. Lange, F. Rebassoo, D. Wright

Lawrence Livermore National Laboratory, Livermore, USA

A. Baden, B. Calvert, S.C. Eno, J.A. Gomez, N.J. Hadley, R.G. Kellogg, T. Kolberg, Y. Lu, M. Marionneau, A.C. Mignerey, K. Pedro, A. Skuja, J. Temple, M.B. Tonjes, S.C. Tonwar

University of Maryland, College Park, USA

A. Apyan, G. Bauer, W. Busza, I.A. Cali, M. Chan, L. Di Matteo, V. Dutta, G. Gomez Ceballos, M. Goncharov, D. Gulhan, M. Klute, Y.S. Lai, A. Levin, P.D. Luckey, T. Ma, S. Nahn, C. Paus, D. Ralph, C. Roland, G. Roland, G.S.F. Stephans, F. Stöckli, K. Sumorok, D. Velicanu, J. Veverka, R. Wolf, B. Wyslouch, M. Yang, Y. Yilmaz, A.S. Yoon, M. Zanetti, V. Zhukova

Massachusetts Institute of Technology, Cambridge, USA

B. Dahmes, A. De Benedetti, A. Gude, S.C. Kao, K. Klapoetke, Y. Kubota, J. Mans, N. Pastika, R. Rusack, A. Singovsky, N. Tambe, J. Turkewitz

University of Minnesota, Minneapolis, USA

J.G. Acosta, L.M. Cremaldi, R. Kroeger, S. Oliveros, L. Perera, R. Rahmat, D.A. Sanders, D. Summers

University of Mississippi, Oxford, USA

E. Avdeeva, K. Bloom, S. Bose, D.R. Claes, A. Dominguez, R. Gonzalez Suarez, J. Keller, I. Kravchenko, J. Lazo-Flores, S. Malik, F. Meier, G.R. Snow

University of Nebraska–Lincoln, Lincoln, USA

J. Dolen, A. Godshalk, I. Iashvili, S. Jain, A. Kharchilava, A. Kumar, S. Rappoccio, Z. Wan

State University of New York at Buffalo, Buffalo, USA

G. Alverson, E. Barberis, D. Baumgartel, M. Chasco, J. Haley, A. Massironi, D. Nash, T. Orimoto, D. Trocino, D. Wood, J. Zhang

Northeastern University, Boston, USA

A. Anastassov, K.A. Hahn, A. Kubik, L. Lusito, N. Mucia, N. Odell, B. Pollack, A. Pozdnyakov, M. Schmitt, S. Stoynev, K. Sung, M. Velasco, S. Won

Northwestern University, Evanston, USA

D. Berry, A. Brinkerhoff, K.M. Chan, M. Hildreth, C. Jessop, D.J. Karmgard, J. Kolb, K. Lannon, W. Luo, S. Lynch, N. Marinelli, D.M. Morse, T. Pearson, M. Planer, R. Ruchti, J. Slaunwhite, N. Valls, M. Wayne, M. Wolf

University of Notre Dame, Notre Dame, USA

L. Antonelli, B. Bylsma, L.S. Durkin, S. Flowers, C. Hill, R. Hughes, K. Kotov, T.Y. Ling, D. Puigh, M. Rodenburg, G. Smith, C. Vuosalo, B.L. Winer, H. Wolfe, H.W. Wulsin

The Ohio State University, Columbus, USA

E. Berry, P. Elmer, V. Halyo, P. Hebda, J. Hegeman, A. Hunt, P. Jindal, S.A. Koay, P. Lujan, D. Marlow, T. Medvedeva, M. Mooney, J. Olsen, P. Piroué, X. Quan, A. Raval, H. Saka, D. Stickland, C. Tully, J.S. Werner, S.C. Zenz, A. Zuranski

Princeton University, Princeton, USA

E. Brownson, A. Lopez, H. Mendez, J.E. Ramirez Vargas

University of Puerto Rico, Mayaguez, USA

E. Alagoz, D. Benedetti, G. Bolla, D. Bortoletto, M. De Mattia, A. Everett, Z. Hu, M. Jones, K. Jung, M. Kress, N. Leonardo, D. Lopes Pegna, V. Maroussov, P. Merkel, D.H. Miller, N. Neumeister, B.C. Radburn-Smith, I. Shipsey, D. Silvers, A. Svyatkovskiy, F. Wang, W. Xie, L. Xu, H.D. Yoo, J. Zablocki, Y. Zheng

Purdue University, West Lafayette, USA

N. Parashar

Purdue University Calumet, Hammond, USA

A. Adair, B. Akgun, K.M. Ecklund, F.J.M. Geurts, W. Li, B. Michlin, B.P. Padley, R. Redjimi, J. Roberts, J. Zabel

Rice University, Houston, USA

B. Betchart, A. Bodek, R. Covarelli, P. de Barbaro, R. Demina, Y. Eshaq, T. Ferbel, A. Garcia-Bellido,
P. Goldenzweig, J. Han, A. Harel, D.C. Miner, G. Petrillo, D. Vishnevskiy, M. Zielinski

University of Rochester, Rochester, USA

A. Bhatti, R. Ciesielski, L. Demortier, K. Goulianos, G. Lungu, S. Malik, C. Mesropian

The Rockefeller University, New York, USA

S. Arora, A. Barker, J.P. Chou, C. Contreras-Campana, E. Contreras-Campana, D. Duggan, D. Ferencek,
Y. Gershtein, R. Gray, E. Halkiadakis, D. Hidas, A. Lath, S. Panwalkar, M. Park, R. Patel, V. Rekovic,
J. Robles, S. Salur, S. Schnetzer, C. Seitz, S. Somalwar, R. Stone, S. Thomas, P. Thomassen, M. Walker

Rutgers, The State University of New Jersey, Piscataway, USA

K. Rose, S. Spanier, Z.C. Yang, A. York

University of Tennessee, Knoxville, USA

O. Bouhali [62], R. Eusebi, W. Flanagan, J. Gilmore, T. Kamon [63], V. Khotilovich, R. Montalvo, I. Osipenkov,
Y. Pakhotin, A. Perloff, J. Roe, A. Safonov, T. Sakuma, I. Suarez, A. Tatarinov, D. Toback

Texas A&M University, College Station, USA

N. Akchurin, C. Cowden, J. Damgov, C. Dragoiu, P.R. Dudero, K. Kovitanggoon, S. Kunori, S.W. Lee,
T. Libeiro, I. Volobouev

Texas Tech University, Lubbock, USA

E. Appelt, A.G. Delannoy, S. Greene, A. Gurrola, W. Johns, C. Maguire, Y. Mao, A. Melo, M. Sharma,
P. Sheldon, B. Snook, S. Tuo, J. Velkovska

Vanderbilt University, Nashville, USA

M.W. Arenton, S. Boutle, B. Cox, B. Francis, J. Goodell, R. Hirosky, A. Ledovskoy, C. Lin, C. Neu, J. Wood

University of Virginia, Charlottesville, USA

S. Gollapinni, R. Harr, P.E. Karchin, C. Kottachchi Kankanamge Don, P. Lamichhane, A. Sakharov

Wayne State University, Detroit, USA

D.A. Belknap, L. Borrello, D. Carlsmith, M. Cepeda, S. Dasu, S. Duric, E. Friis, M. Grothe, R. Hall-Wilton,
M. Herndon, A. Hervé, P. Klabbers, J. Klukas, A. Lanaro, R. Loveless, A. Mohapatra, I. Ojalvo, T. Perry,
G.A. Pierro, G. Polese, I. Ross, T. Sarangi, A. Savin, W.H. Smith, J. Swanson

University of Wisconsin, Madison, USA

[†] Deceased.
[1] Also at Vienna University of Technology, Vienna, Austria.
[2] Also at CERN, European Organization for Nuclear Research, Geneva, Switzerland.
[3] Also at Institut Pluridisciplinaire Hubert Curien, Université de Strasbourg, Université de Haute Alsace Mulhouse, CNRS/IN2P3, Strasbourg, France.
[4] Also at National Institute of Chemical Physics and Biophysics, Tallinn, Estonia.
[5] Also at Skobeltsyn Institute of Nuclear Physics, Lomonosov Moscow State University, Moscow, Russia.
[6] Also at Universidade Estadual de Campinas, Campinas, Brazil.
[7] Also at California Institute of Technology, Pasadena, USA.
[8] Also at Laboratoire Leprince-Ringuet, Ecole Polytechnique, IN2P3–CNRS, Palaiseau, France.
[9] Also at Zewail City of Science and Technology, Zewail, Egypt.
[10] Also at Suez Canal University, Suez, Egypt.
[11] Also at Cairo University, Cairo, Egypt.
[12] Also at Fayoum University, El-Fayoum, Egypt.
[13] Also at British University in Egypt, Cairo, Egypt.
[14] Now at Ain Shams University, Cairo, Egypt.
[15] Also at National Centre for Nuclear Research, Swierk, Poland.

[16] Also at Université de Haute Alsace, Mulhouse, France.
[17] Also at Universidad de Antioquia, Medellin, Colombia.
[18] Also at Joint Institute for Nuclear Research, Dubna, Russia.
[19] Also at Brandenburg University of Technology, Cottbus, Germany.
[20] Also at The University of Kansas, Lawrence, USA.
[21] Also at Institute of Nuclear Research ATOMKI, Debrecen, Hungary.
[22] Also at Eötvös Loránd University, Budapest, Hungary.
[23] Also at Tata Institute of Fundamental Research – EHEP, Mumbai, India.
[24] Also at Tata Institute of Fundamental Research – HECR, Mumbai, India.
[25] Now at King Abdulaziz University, Jeddah, Saudi Arabia.
[26] Also at University of Visva-Bharati, Santiniketan, India.
[27] Also at University of Ruhuna, Matara, Sri Lanka.
[28] Also at Isfahan University of Technology, Isfahan, Iran.
[29] Also at Sharif University of Technology, Tehran, Iran.
[30] Also at Plasma Physics Research Center, Science and Research Branch, Islamic Azad University, Tehran, Iran.
[31] Also at Università degli Studi di Siena, Siena, Italy.
[32] Also at Centre National de la Recherche Scientifique (CNRS) – IN2P3, Paris, France.
[33] Also at Purdue University, West Lafayette, USA.
[34] Also at Universidad Michoacana de San Nicolas de Hidalgo, Morelia, Mexico.
[35] Also at Faculty of Physics, University of Belgrade, Belgrade, Serbia.
[36] Also at Facoltà Ingegneria, Università di Roma, Roma, Italy.
[37] Also at Scuola Normale e Sezione dell'INFN, Pisa, Italy.
[38] Also at University of Athens, Athens, Greece.
[39] Also at Paul Scherrer Institut, Villigen, Switzerland.
[40] Also at Institute for Theoretical and Experimental Physics, Moscow, Russia.
[41] Also at Albert Einstein Center for Fundamental Physics, Bern, Switzerland.
[42] Also at Gaziosmanpasa University, Tokat, Turkey.
[43] Also at Adiyaman University, Adiyaman, Turkey.
[44] Also at Cag University, Mersin, Turkey.
[45] Also at Mersin University, Mersin, Turkey.
[46] Also at Izmir Institute of Technology, Izmir, Turkey.
[47] Also at Ozyegin University, Istanbul, Turkey.
[48] Also at Kafkas University, Kars, Turkey.
[49] Also at Suleyman Demirel University, Isparta, Turkey.
[50] Also at Ege University, Izmir, Turkey.
[51] Also at Mimar Sinan University, Istanbul, Istanbul, Turkey.
[52] Also at Kahramanmaras Sütcü Imam University, Kahramanmaras, Turkey.
[53] Also at Rutherford Appleton Laboratory, Didcot, United Kingdom.
[54] Also at School of Physics and Astronomy, University of Southampton, Southampton, United Kingdom.
[55] Also at INFN Sezione di Perugia; Università di Perugia, Perugia, Italy.
[56] Also at Utah Valley University, Orem, USA.
[57] Also at Institute for Nuclear Research, Moscow, Russia.
[58] Also at University of Belgrade, Faculty of Physics and Vinca Institute of Nuclear Sciences, Belgrade, Serbia.
[59] Also at Argonne National Laboratory, Argonne, USA.
[60] Also at Erzincan University, Erzincan, Turkey.
[61] Also at Yildiz Technical University, Istanbul, Turkey.
[62] Also at Texas A&M University at Qatar, Doha, Qatar.
[63] Also at Kyungpook National University, Daegu, Republic of Korea.